NIPER-482
Distribution Category UC-125

THE THERMODYNAMIC PROPERTIES OF 2-AMINOBIPHENYL

Topical Report

NIPER--482

DE91 002209

By
W. V. Steele
R. D. Chirico
S. E. Knipmeyer
A. Nguyen

December 1990

Work Performed Under Cooperative Agreement No. DE-FC22-83FE60149

Prepared for
U.S. Department of Energy
Assistant Secretary for Fossil Energy

W. D. Peters, Project Manager
Bartlesville Project Office
P.O. Box 1398
Bartlesville, OK 74005

Prepared by
IIT Research Institute
National Institute for Petroleum and Energy Research
P.O. Box 2128
Bartlesville, OK 74005

EXECUTIVE SUMMARY

Catalytic hydrodenitrogenation (HDN) is a key step in upgrading processes for conversion of heavy petroleum, shale oil, tar sands, and the products of the liquefaction of coal to economically viable products. Organic nitrogen and sulfur are commonly removed via reaction at 300 to 400° C and 50 to 150 atm. of hydrogen. Under these severe conditions, hydrogen is consumed not only in breaking carbon-nitrogen and carbon-sulfur bonds, but also in saturating aromatic components in the feed. Hydrogen consumption in excess of 1500 scf/bbl (standard cubic feet per barrel) is common in hydrotreating shale oil, while the amount theoretically required for selective heteroatom removal is only about 600 scf/bbl. The problem is exacerbated as the number of rings in nitrogen and sulfur-containing molecules is increased. Hence, the saving in expensive hydrogen could be enormous, if a process for denitrogenation without saturation of the aromatic rings in the feedstock could be developed.

This research program, funded by the Department of Energy (DOE) Office of Fossil Energy, Advanced Extraction and Process Technology (AEPT), provides accurate experimental thermochemical and thermophysical properties for "key" organic nitrogen-containing compounds present in the range of alternative feedstocks, and applies the experimental information to thermodynamic analyses of key HDN reaction networks (e.g., quinoline/hydrogen, indole/hydrogen, acridine/hydrogen, etc.). Thermodynamic analyses, based on accurate information, can be used to set the boundaries (e.g., temperature range, pressure range, etc.) for efficient processing of materials, and to provide insights for the design of cost-effective methods of nitrogen removal.

Previous reports by this research group have discussed the two-ring systems; indole/H_2 and quinoline/H_2. This report is the first in a series that will lead to an analysis of a three-ring HDN system; the carbazole/hydrogen reaction network. 2-Aminobiphenyl is the initial intermediate in the HDN pathway for carbazole, which consumes the least hydrogen possible. In this report, thermodynamic-property measurements for this molecule are detailed, and the results are used in thermodynamic calculations to compare the feasibility of the initial hydrogenolysis step in the carbazole/H_2 network with that of its hydrocarbon and oxygen-containing analogues; i.e., fluorene/H_2 and dibenzofuran/H_2.

Results of the thermodynamic calculations are compared with those of batch-reaction studies reported in the literature. The "crossover temperature" concept is shown to be a valuable tool in the interpretation of the reaction-study results, and the thermodynamic calculations and reaction studies are found to be in accord. For the hydrodenitrogenation of carbazole, the reaction pathway using the minimum of hydrogen (carbazole → 2-aminobiphenyl → biphenyl) probably cannot be realized, but the

pathway (carbazole → 2-aminobiphenyl → 2-phenylcyclohexylamine → cyclohexylbenzene) should be possible with proper catalyst selection.

The report concludes that if minimization of hydrogen consumption is the goal of hydroprocessing of liquids containing compounds with carbazole and/or dibenzofuran moieties present, then catalysts other than those used in present refineries will be required. However, as was noted in the previous topical report on the hydrodenitrogenation of quinoline (NIPER-468), the presence of sulfur compounds in the processing liquid will restrict the operation of such a catalyst. Upgrading of such liquids will require new processing technology such as "Staged Upgrading." Staged Upgrading, as used in this context, is where different compound types are removed under conditions which favor their individual removal. For example, remove sulfur compounds first followed by nitrogen compounds under a completely different set of conditions of catalyst, hydrogen pressure, and temperature. This concept will be the subject of a future topical report from this group.

ABSTRACT

Measurements leading to the calculation of the ideal-gas thermodynamic properties for 2-aminobiphenyl are reported. Experimental methods included combustion calorimetry, adiabatic heat-capacity calorimetry, comparative ebulliometry, inclined-piston gauge manometry, and differential-scanning calorimetry (d.s.c.). Entropies, enthalpies, and Gibbs energies of formation were derived for the ideal gas for selected temperatures between 298.15 K and 820 K. The critical temperature and critical density were determined for 2-aminobiphenyl with the d.s.c., and the critical pressure was derived. The Gibbs energies of formation are used in thermodynamic calculations to compare the feasibility of the initial hydrogenolysis step in the carbazole/H_2 network with that of its hydrocarbon and oxygen-containing analogues; i.e., fluorene/H_2 and dibenzofuran/H_2. Results of the thermodynamic calculations are compared with those of batch-reaction studies reported in the literature.

ACKNOWLEDGEMENTS

The authors gratefully acknowledge the financial support of the Office of Fossil Energy of the U.S. Department of Energy. This research was funded within the Advanced Extraction and Process Technology (AEPT) program as part of the Cooperative Agreement DE–FC22-83FE60149.

The authors acknowledge Professor E. J. "Pete" Eisenbraun and his research group at Oklahoma State University for preparation of the samples, and the assistance of I. A. Hossenlopp in vapor-transfer of the materials prior to the calorimetric measurements.

TABLE OF CONTENTS

TABLE OF CONTENTS (continued)

LIST OF TABLES

LIST OF FIGURES

GLOSSARY

This report is written with close adherence to the style adopted by The Journal of Chemical Thermodynamics. A complete description of the style can be found in the January 1990 issue of the Journal of Chemical Thermodynamics. This glossary summarizes the main points with respect to the symbol usage.

Throughout this report only SI units are used in reporting thermodynamic values. All values are given in dimensionless units i.e., physical quantity = number X unit; for example $\rho/(kg \cdot m^{-3})$ rather than " ρ (kg/m^3)" or " ρ kg/m^3". Molar values, i.e., intensive functions, are denoted by the subscript "m", e.g., $C_{sat,m}$, whereas extensive functions do not have the subscript. In addition, since thermodynamic values are pressure dependent, they are reported in terms of a standard pressure p°, which in this report is 101.325 kPa (one atmosphere).

M = molar mass in $g \cdot mol^{-1}$

T = temperature in Kelvin

p = pressure in Pascals (Pa)

ρ = density in $kg \cdot m^{-3}$

$\Delta_c U^\circ_m$ = molar energy of combustion

$\Delta_c U^\circ_m/M$ = energy of combustion per gram

$\Delta_c H^\circ_m$ = molar enthalpy of combustion

$\Delta_f H^\circ_m$ = molar enthalpy of formation

$\Delta^g_l H_m$ = molar enthalpy of vaporization, hence the subscript l (for liquid) and superscript g (for gas)

$\Delta^g_l V_m$ = change in molar volume from the liquid to the real vapor

$C_{v,m}$ = molar heat capacity at constant volume

$C_{p,m}$ = molar heat capacity at constant pressure

$C_{sat,m}$ = molar heat capacity at saturated pressure

μ = chemical potential

n = number of moles of substance

V_x = volume of d.s.c. cell at a temperature T/K.

C^{II}_x = two-phase heat capacity at cell volume V_x

C^{II}_V = two-phase heat capacity at constant volume

$C^{II}_V (\rho = \rho_{sat})$ = two-phase heat capacity along the saturation line

V_l = molar volume of the liquid

T_c = critical temperature

p_c = critical pressure

ρ_c = critical density

T_r = reduced temperature = T/T_c

p_r = reduced pressure = p/p_c

ρ_r = reduced density = ρ/ρ_c

lg = $\log_{10}$

ω = acentric factor = [-lg (p_x/p_c) - 1]; p_x is the vapor pressure at T_r = 0.7

$\Delta_0^T S_m^o$ = molar entropy at temperature T/K (relative to the entropy at T=0 K)

$\Delta_0^T H_m^o$ = molar enthalpy at temperature T/K (relative to the crystals at 0 K)

$\Delta_{comp} S_m$ = molar entropy of compression of a gas

$\Delta_{imp} S_m$ = gas imperfection term

$T \rightarrow 0$ = Zero Kelvin

To avoid listing units in tables, entropies are reported as divided by the gas constant R, and enthalpies and Gibbs energies are generally reported divided by the product of the gas constant and temperature, R·T. Units of time are s (seconds) or h (hours).

1. INTRODUCTION

In this research program, funded by the Department of Energy (DOE) Office of Fossil Energy, Advanced Extraction and Process Technology (AEPT), thermochemical and thermophysical properties are determined for "key" organic nitrogen-containing compounds present in heavy petroleum, shale oil, tar sands, and the products of the liquefaction of coal. Catalytic hydrodenitrogenation (HDN) is a key step in the upgrading of these feedstocks.[1-4]§ They are typically rich in nitrogen, and their fractionation produces distillates that are also rich in nitrogen, thus giving poor quality distillate fuels without denitrogenation.

Hydrodenitrogenation (HDN) reaction systems for aromatic compounds contain steps where the aromatic ring structures are hydrogenated. These reaction steps are all reversible within the temperature and pressure ranges of hydrogenation reactors used commercially. Therefore, a knowledge of the thermodynamic equilibria among the species is necessary for the proper interpretation of reaction data, for comparing different catalysts, and for accurate modelling of the overall reaction. In addition a knowledge of thermophysical properties, particularly the critical temperature, critical volume, and critical pressure, is necessary for process-design estimations.

Oversaturation of rings is a common problem in the HDN of aromatic compounds. Therefore, to minimize consumption of expensive hydrogen in processing, the HDN pathway involving the most efficient use of hydrogen is sought. The problem of oversaturation in the HDN of aromatics is exacerbated as the number of rings increases. This research group has reported thermodynamic analyses of the indole/hydrogen[5] and quinoline/hydrogen[6] networks. This report is the first in a series that will lead to an analysis of a three-ring system; the carbazole/hydrogen HDN network.

2-Aminobiphenyl is the initial intermediate in the HDN pathway for carbazole, which consumes the least hydrogen possible. In this report, thermodynamic-property measurements for this molecule are detailed, and the results are used to compare the thermodynamic feasibility of the initial hydrogenolysis step in the carbazole/H_2 network with that of its hydrocarbon and oxygen-containing analogues; i.e., fluorene/H_2 and dibenzofuran/H_2.

---

§ References are listed in numerical order at the end of this Report.

2. EXPERIMENTAL

MATERIALS

A commercial sample of 2-aminobiphenyl was purified in the following manner. The impure sample was treated with oxalic acid dihydrate in propan-2-ol at 353 K (molecular proportions 1.4 to 1 to 50 for 2-aminobiphenyl, oxalic acid dihydrate, and propan-2-ol, respectively). The resulting oxalate was twice recrystallized from propan-2-ol/water (molar ratio 4:1), and cleaved using 2 $mol \cdot dm^{-3}$ KOH(aq). The liberated 2-aminobiphenyl was extracted with ether, dried (Na_2CO_3), filtered, and concentrated. Final purification was achieved by double distillation at 383 K and 200 Pa.

The mole-fraction impurities were estimated to be <0.001 for 2-aminobiphenyl using d.s.c. purity analysis techniques. The high purity of the calorimetric sample was confirmed both in fractional-melting studies completed as part of the adiabatic heat-capacity studies and the small differences observed between the boiling and condensation temperatures in the ebulliometric vapor-pressure measurements. The mole-fraction of impurities determined in the fractional-melting studies was 0.00024.

The water used as a reference material in the ebulliometric vapor-pressure measurements was deionized and distilled from potassium permanganate. The decane used as a reference material for the ebulliometric measurements was purified by urea complexation, two recrystallizations of the complex, its decomposition with water, extraction with ether, drying with $MgSO_4$, and distillation at 337 K and 1 kPa pressure.

PHYSICAL CONSTANTS AND STANDARDS

Molar values are reported in terms of M = 169.226 $g \cdot mol^{-1}$ for 2-aminobiphenyl based on the relative atomic masses of 1981[7]† and the gas constant, R = 8.31451 $J \cdot K^{-1} \cdot mol^{-1}$, adopted by CODATA.[8] The platinum resistance thermometers used in these measurements were calibrated by comparison with standard thermometers whose constants were determined at the National Institute of Standards and Technology (NIST), formerly the National Bureau of Standards (NBS). All temperatures reported are in terms of the IPTS-68.[9] The platinum resistance thermometer used in the adiabatic heat-capacity studies was calibrated below 13.81 K using the method of McCrackin and Chang.[10] Measurements of mass, time, electrical resistance, and potential difference were made in terms of standards traceable to calibrations at NIST.

---

† The 1981 relative atomic masses were used because the CODATA Recommended Key Values for Thermodynamics (reference 30) are based on them.

APPARATUS AND PROCEDURES

Combustion Calorimetry. The experimental procedures used in the combustion calorimetry of organic nitrogen compounds at the National Institute for Petroleum and Energy Research have been described.[11-13] A rotating-bomb calorimeter (laboratory designation ERM II)[14] and platinum-lined bomb (laboratory designation Pt-3b)[15] with an internal volume of 0.3934 dm^3 were used without rotation. 2-Aminobiphenyl was burned in the form of pellets. For each experiment 1.0×10^{-3} dm^3 of water was added to the bomb, and the bomb was flushed and charged to 3.04 MPa with pure oxygen. Judicious choice of sample and auxiliary masses allowed the temperature rise in each combustion series and its corresponding calibration series to be the same within 0.1 per cent. All experiments were completed within 0.01 K of 298.15 K.

Temperatures were measured by quartz-crystal thermometry.[16,17] A computer was used to control the combustion experiments and record the results. The quartz-crystal thermometer was calibrated by comparison with a platinum resistance thermometer. Counts of the crystal oscillation were taken over periods of 100 s throughout the experiments. Integration of the time-temperature curve is inherent in the quartz-crystal thermometer readings.[18]

NBS benzoic acid (sample 39i) was used for calibration of the calorimeter; its specific energy of combustion is $-(26434.0 \pm 3.0)$ $J \cdot g^{-1}$ under certificate conditions. Conversion to standard states[19] gives $-(26413.7 \pm 3.0)$ $J \cdot g^{-1}$ for $\Delta_c U^\circ_m/M$, the specific energy of the idealized combustion reaction. Calibration experiments were interspersed with the 2-aminobiphenyl measurements. Nitrogen oxides were not formed in the calibration experiments due to the high purity of the oxygen used and preliminary bomb flushing. The energy equivalent of the calorimeter obtained for the calibration series, ε(calor), was (16770.7 ± 0.5) $J \cdot K^{-1}$ (mean and standard deviation of the mean). For the cotton fuse, empirical formula $CH_{1.774}O_{0.887}$, $\Delta_c U^\circ_m/M$ was -16945 $J \cdot g^{-1}$.

Auxiliary information, necessary for reducing weights measured in air to masses, converting the energy of the actual bomb process to that of the isothermal process, and reducing to standard states,[19] included a density at 298.15 K of 1012 $kg \cdot m^{-3}$ and an estimated value of 5×10^{-7} $m^3 \cdot K^{-1}$ for $(\delta V_m/\delta T)_p$ for 2-aminobiphenyl. The density was obtained by weighing a pellet of known volume. The molar heat capacity at 298.15 K for 2-aminobiphenyl used in the corrections to standard states is given as part of the heat-capacity study results later in this report.

Nitric acid formed during the 2-aminobiphenyl combustions was determined by titration with standard sodium hydroxide.[20] Carbon dioxide was also recovered from

the combustion products of each experiment. Anhydrous lithium hydroxide was used as absorbent.[12] The combustion products were checked for unburned carbon and other products of incomplete combustion, but none were detected. Carbon dioxide percentage recoveries were 99.992±0.014 (mean and standard deviation of the mean) for the calibrations and 99.992±0.004 for the corresponding 2-aminobiphenyl combustions.

Ebulliometric Vapor-Pressure Measurements. The essential features of the ebulliometric equipment and procedures are described in the literature.[21,22] The ebulliometers were used to reflux the substance under study with a standard of known vapor pressure under a common helium atmosphere. The boiling and condensation temperatures of the two substances were determined, and the vapor pressure was derived using the condensation temperature of the standard.[23]

The precision in the temperature measurements for the ebulliometric vapor-pressure studies was 0.001 K. Uncertainties in the pressures are adequately described by:

$$\sigma(p) = (0.001\ \mathrm{K})\{(dp_{ref}/dT)^2 + (dp_x/dT)^2\}^{1/2}, \qquad (2)$$

where p_{ref} is the vapor pressure of the reference substance and p_x is the vapor pressure of the sample under study. Values of dp_{ref}/dT for the reference substances were calculated from fits of the Antoine equation[24] to vapor pressures of the reference materials (decane and water) reported in reference 23.

Inclined-Piston Vapor-Pressure Measurements. The equipment for these measurements has been described by Douslin and McCullough,[25] and Douslin and Osborn.[26] Recent revisions to the equipment and procedures have been reported.[27] The low pressure range of the inclined-piston measurements, 10 to 3500 Pa, necessitated diligent outgassing of the sample prior to introduction into the apparatus. Also, prior to the sample introduction, all parts of the cell in contact with the sample were baked at 623 K under high vacuum (< 10^{-4} Pa). The thoroughly outgassed samples were placed in the apparatus, and additional outgassing was performed prior to commencing measurements. Finally, prior to each measurement, a small amount of sample was pumped off. Measurements were made as a function of time to extrapolate the pressure to the time when the pumping valve was closed; i.e., to the time when insignificant amounts of light gas had leaked into the system or diffused out of the sample.

Uncertainties in the pressures determined with the inclined-piston apparatus, on the basis of estimated precision of measuring the mass, area, and angle of inclination of the piston, are adequately described by the expression:

$$\sigma(p) = 1.5\times10^{-4}p + 0.2 \text{ Pa.} \qquad (3)$$

The uncertainties in the temperatures are 0.001 K.

Adiabatic Heat-Capacity Calorimetry. Adiabatic heat-capacity and enthalpy measurements were made with a calorimetric system described previously.[27] The calorimeter characteristics and sealing conditions are given in table 1.¶ Energy measurement procedures were the same as those described for studies on quinoline.[27] Thermometer resistances were measured with self-balancing alternating-current resistance bridges (H. Tinsley & Co. Ltd.; Models 5840C and 5840D). Energies were measured to a precision of 0.01 per cent, and temperatures were measured to a precision of 0.0001 K. The energy increments to the filled calorimeter were corrected for enthalpy changes in the empty calorimeter, for the helium exchange gas, and for vaporization of the sample. The maximum correction to the measured energy for the helium exchange gas was 0.1 per cent near 5 K. The sizes of the other two corrections are indicated in table 1.

Differential-Scanning Calorimetry (d.s.c.). Differential-scanning calorimetric measurements were made with a Perkin-Elmer DSC-2. Experimental methods were described previously.[28]

3. RESULTS

COMBUSTION CALORIMETRY

A typical combustion experiment for 2-aminobiphenyl is summarized in table 2. It is impractical to list summaries for each combustion, but values of $\Delta_c U^\circ_m/M$ for all the experiments are reported in table 3. All values of $\Delta_c U^\circ_m/M$ in table 3 refer to the reaction:

$$C_{12}H_{11}N \text{ (cr)} + 14.75\ O_2 \text{ (g)} = 12\ CO_2 \text{ (g)} + 5.5\ H_2O \text{ (l)} + 1/2\ N_2 \text{ (g)}. \qquad (4)$$

Table 3 also gives derived values of the standard molar energy of combustion $\Delta_c U^\circ_m$, the standard molar enthalpy of combustion $\Delta_c H^\circ_m$, and the standard molar enthalpy of

¶ All tables are given at the end of this report.

formation $\Delta_f H^o_m$ for 2-aminobiphenyl. Values of $\Delta_c U^o_m$ and $\Delta_c H^o_m$ refer to reaction **4**. The values of $\Delta_f H^o_m$ refer to reaction **5**:

$$12\ C(cr,\ graphite) + 5.5\ H_2\ (g) + 1/2\ N_2\ (g) = C_{12}H_{11}N\ (cr\ or\ l). \qquad (5)$$

Uncertainties given in table 3 are the "uncertainty interval" defined in reference 29. The enthalpies of formation of $CO_2(g)$ and $H_2O(l)$ were taken to be $-(393.51\pm0.13)$ and $-(285.830 \pm 0.042)$ $kJ \cdot mol^{-1}$, respectively, as assigned by CODATA.[30]

VAPOR-PRESSURE MEASUREMENTS

Vapor pressures for 2-aminobiphenyl are reported in table 4. Following previous practice,[22] the results obtained in the ebulliometric measurements were adjusted to common pressures. The common pressures, the condensation temperatures, and the difference between condensation and boiling temperatures for the samples are reported. The small differences between the boiling and condensation temperatures for 2-aminobiphenyl indicated correct operation of the equipment and the high purity of the samples.

Cox Equation Fits to Vapor Pressures. Previous studies by Scott and Osborn[31] showed that the Cox equation[32] can represent measured vapor pressures adequately from the triple-point pressure to 0.3 MPa. Scott and Osborn also showed that the Antoine equation, the most commonly used to represent vapor pressures, does not extrapolate well outside the experimental range. In contrast, the Cox equation extrapolates with reasonable precision over a 50 K range.[31]

The Cox equation in the form:

$$\ln(p/p_{ref}) = \{1 - (T_{ref}/T)\}\exp\{A + B(T/K) + C(T/K)^2\}\ , \qquad (6)$$

was fitted to the experimental vapor pressures with p_{ref} chosen to be 101.325 kPa so that T_{ref} was the normal-boiling temperature. In those fits, the sums of the weighted squares in the function:

$$\Delta = \ln\{\ln(p/p_{ref})/(1 - T_{ref}/T)\} - A - B(T/K) - C(T/K)^2\ , \qquad (7)$$

were minimized. The weighting factors W, the reciprocals of the variance in Δ derived from the propagation of errors in the temperature and pressure determinations, are defined by:

$$1/W = (\delta\Delta/\delta T)^2_p\, \sigma(T)^2 + (\delta\Delta/\delta p)^2_T\, \sigma(p)^2\ . \qquad (8)$$

Parameters derived from the fits are given in table 5. Details of the Cox equation fits are given in table 4.

Derived Enthalpies of Vaporization. Enthalpies of vaporization $\Delta_l^g H_m$ were derived from the Cox equation fits using the Clapeyron equation:

$$dp/dT = \Delta_l^g H_m / (T \Delta_l^g V_m) , \qquad (9)$$

where $\Delta_l^g V_m$ is the increase in molar volume from the liquid to the real vapor. Estimates of second virial coefficients and liquid-phase densities were made with the extended corresponding-states equation of Pitzer and Curl,[33] as formulated by Hales and Townsend.[34] Third virial coefficients were estimated with the corresponding-states method of Orbey and Vera.[35] This formulation for the third virial coefficient was applied successfully in analyses of the thermodynamic properties of benzene, toluene, and decane.[36] The third virial coefficient is required for accurate calculation of the gas volume for pressures greater than one bar. Derived enthalpies of vaporization and entropies of compression are reported in table 6.

ADIABATIC HEAT-CAPACITY CALORIMETRY

Crystallization and Melting Studies. Crystallization of 2-aminobiphenyl was initiated by slowly cooling (approximately 2.5 $mK \cdot s^{-1}$) the liquid sample 35 to 40 K below the triple-point temperature. Complete crystallization was ensured by maintaining the sample under adiabatic conditions in the partially melted state (15 to 25 per cent liquid) until ordering of the crystals was complete, as evidenced by a cessation of spontaneous warming. The sample warmed for approximately 8 h following the partial remelting. The sample was cooled at an effective rate of 3 $mK \cdot s^{-1}$ to crystallize the remaining liquid. As a final step, the sample was thermally cycled between <200 K and within 2 K of the triple-point temperature, where it was held for a minimum of 24 h to provide further tempering. All of the solid-phase measurements were performed upon crystals pre-treated in this manner.

The triple-point temperature T_{tp} and sample purity were determined by measurement of the equilibrium melting temperatures T(F) as a function of fraction F of the sample in the liquid state.[37] Equilibrium melting temperatures were determined by measuring temperatures at approximately 300-s intervals for 0.75 to 1 h after an energy input and extrapolating to infinite time by assuming an exponential decay toward the equilibrium value. The observed temperatures at 1 h after an energy input were

invariably within 3 mK of the calculated equilibrium temperatures for F values listed in table 7. No evidence for solid-soluble impurities was found.

Phase Transformations and Enthalpy Measurements. Experimental molar enthalpy results are summarized in table 8. The table includes both phase-transition enthalpies and single-phase measurements, which serve as checks on the integration of the heat-capacity results. Corrections for pre-melting caused by impurities were made in these evaluations. Results with the same series number in tables 8 and 9 were taken without interruption of adiabatic conditions.

Excellent reproducibility (within ±0.02 per cent) was obtained in the enthalpy-of-fusion results. This implies that phase cr(I) was formed reproducibly by means of the tempering methods described above. The sample showed a single solid-phase transition near 258 K with little associated enthalpy. Prior to measurements of the transition enthalpy, the sample was annealed between 255 and 258 K for 45, 80, and 150 h for series 6, 10, and 13, respectively. No warming was detected for crystals annealed for longer than approximately 48 h. This is in accord with the results shown in table 8. The measured transition enthalpies for series 10 and 13 are nearly identical, while that for series 6 is slightly low. The series 6 results were not used in the calculation of the average transition enthalpy.

Heat Capacity Measurements. The experimental molar heat capacities under vapor saturation pressure $C_{sat,m}$ determined by adiabatic calorimetry are listed in table 9. Values in table 9 were corrected for effects of sample vaporization into the gas space of the calorimeter. The temperature increments were small enough to obviate the need for corrections for non-linear variation of $C_{sat,m}$ with temperature except near the solid-phase transition temperature. The precision of the heat-capacity measurements ranged from approximately 5 per cent at 5 K, to 2 per cent at 11 K, 0.2 per cent near 20 K, and improved gradually to less than 0.1 per cent above 100 K, except in the solid phase near the triple-point and solid-phase transition temperature where equilibration times were long. The heat capacities in table 9 have not been corrected for pre-melting, but from the temperature increments provided an independent calculation can be made. The curve of heat capacity against temperature is shown in figure 1. Results above 450 K were determined by d.s.c. as described later in this report.

For heat-capacity measurements in the liquid phase, equilibrium was reached in less than 1 h. Equilibration times for phase cr(II) were less than 1 h for temperatures below 240 K, and increased to 2 h at 245 K, 4 h at 250 K, and 12 h

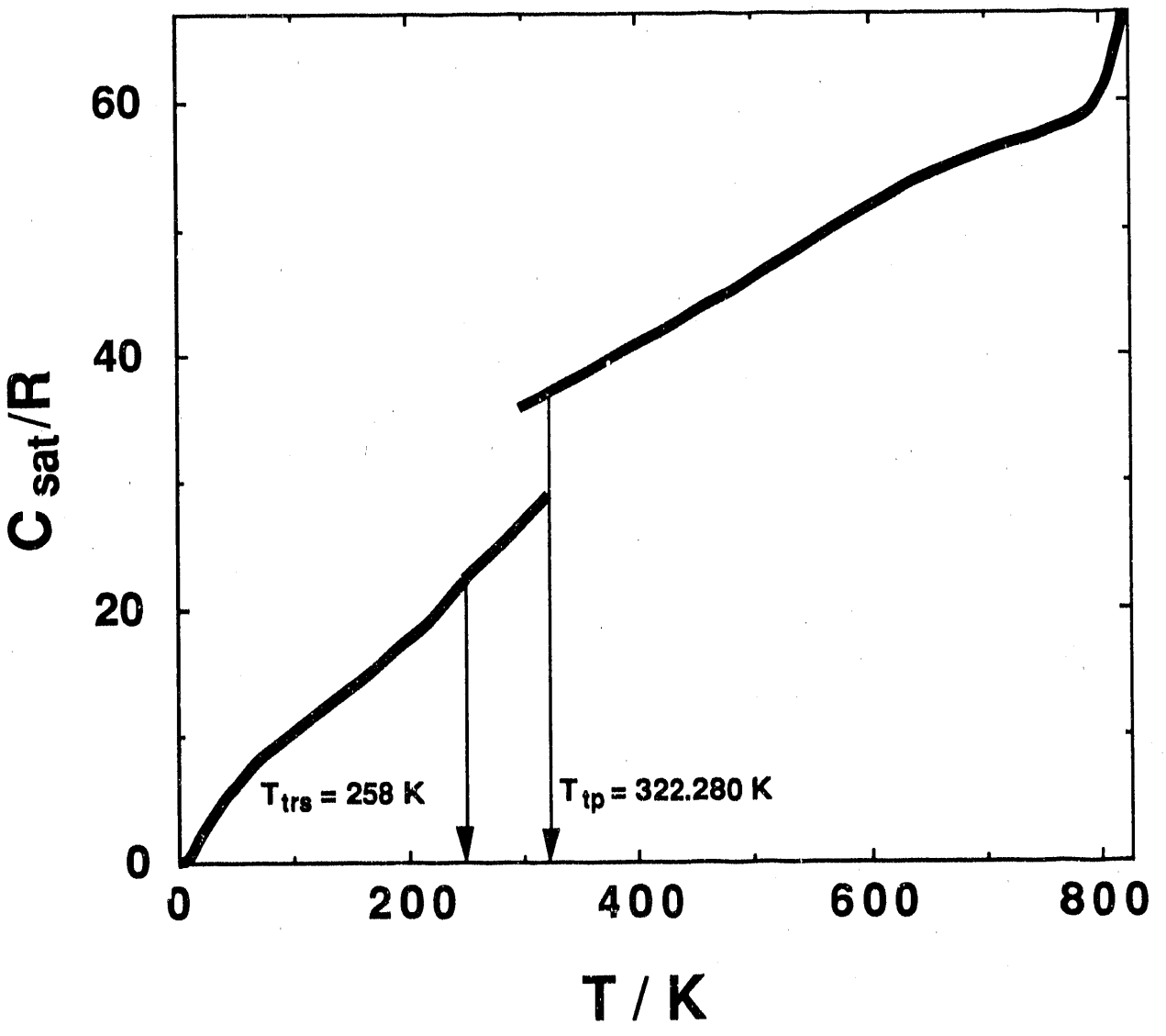

Figure 1. Heat-capacity-against-temperature curve for 2-aminobiphenyl. The vertical lines indicate phase-transition temperatures.

at 255 K. For phase cr(I), equilibration times were approximately 9 h and were independent of temperature. Details of the heat-capacity measurements in the cr(II)-to-cr(I) transition region are shown in figure 2. The uninterrupted curve was drawn to be consistent with these results. (Heat-capacity values sufficient to define this curve are included in table 10.) The transition temperature was determined to within approximately ±2 K. The uncertainty in this value does not affect significantly the derived entropies. Extrapolation of the heat-capacity results to $T \rightarrow 0$ was made by linear extrapolation of a plot of $C_{sat,m}/T$ against temperature squared for results below 10 K.

DIFFERENTIAL SCANNING CALORIMETRY

Theoretical Background. The theoretical background for the determination of heat capacities at vapor-saturation pressure, $C_{sat,m}$, with results obtained with a d.s.c. has been described.[32] If two phases are present and the liquid is a pure substance, then the vapor pressure p and the chemical potential μ are independent of the amount of substance n and the cell volume V_x, and are equal to p_{sat} and μ_{sat}. The two-phase heat capacities at cell volume V_x, $C^{II}_{x,m}$, can be expressed in terms of the temperature derivatives of these quantities:

$$n\,C^{II}_{x,m}/T = -n(\delta^2\mu/\delta T^2)_{sat} + V_x\,(\delta^2 p/\delta T^2)_{sat} + \{(\delta V_x/\delta T)_x\,(\delta p/\delta T)_{sat}\} \quad (10)$$

The third term on the right-hand side of equation (**10**) includes the thermal expansion of the cell. In this research the thermal expansion of the cells was expressed as:

$$V_x(T) \,/\, V_x(298.15\ K) = 1 + ay + by^2, \quad (11)$$

where, $y = (T - 298.15)$ K, $a = 3.216 \times 10^{-5}$ K^{-1}, and $b = 5.4 \times 10^{-8}$ K^{-2}.

$(\delta p/\delta T)_{sat}$ can be calculated based on the vapor pressures measured in this research. Therefore, with a minimum of two different filling levels of the cell $(\delta^2 p/\delta T^2)_{sat}$ and $(\delta^2\mu/\delta T^2)_{sat}$ can be determined. In this research three fillings were used. To obtain the saturation heat capacity $C_{sat,m}$ at vapor pressures greater than 0.1 MPa, the limit where the cell is full of liquid is required; i.e., $(n/V_x) = \{1/V_m(l)\}$ where $V_m(l)$ is the molar volume of the liquid:

$$\lim_{(n/V_x) \rightarrow \{1/V_m(l)\}} (n\,C^{II}_{v,m}/T) = V_m(l)(\delta^2 p/\delta T^2)_{sat} - n(\delta^2\mu/\delta T^2)_{sat}. \quad (12)$$

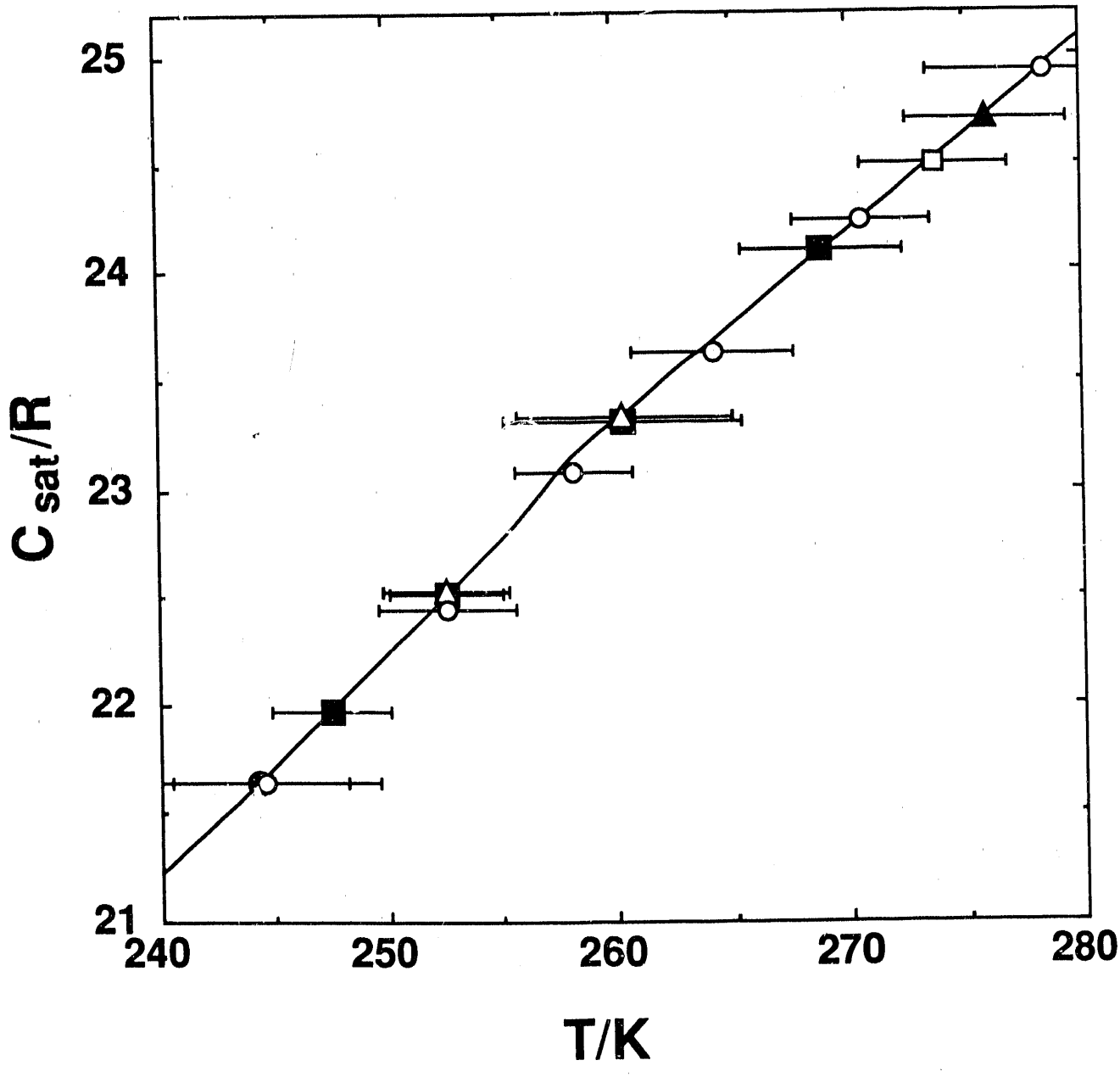

Figure 2. Experimental average heat capacities in the cr(II)-to-cr(I) transition region for 2-aminobiphenyl. □, series 5; ○, series 6; ▲, series 7; ■, series 10; ●, series 11; △, series 13. The horizontal bars span the temperature increment associated with each average heat-capacity value. The heat-capacity curve is described in the text.

$C_{sat,m}$ is obtained using the expression:

$$\lim_{(n/V_x) \rightarrow \{1/V_m(l)\}} (n\, C^{II}_{V,m}) = n[C_{sat,m} - \{T(\delta p/\delta T)_{sat}\, (dV_m(l)/dT)\}]. \quad (13)$$

Thus, reliable liquid density values are also required to determine $C_{sat,m}$.

d.s.c. Measurement Results. Table 11 lists the experimental two-phase heat capacities $C^{II}_{x,m}$ for 2-aminobiphenyl obtained for three cell fillings. Heat-capacities were determined at 20-K intervals with a heating rate of 0.083 $K \cdot s^{-1}$ and a 120 s equilibration period between heats. Sample decomposition precluded heat-capacity measurements above 800 K.

By employing a single continuous heat at a heating rate of 0.333 $K \cdot s^{-1}$, sample decomposition was greatly reduced, and the abrupt decrease in heat capacity associated with the conversion from the two-phases to one-phase was observed. Temperatures at which conversion to the single phase occurred were measured in this way for six cell fillings. Table 12 reports the density, obtained from the mass of sample and the cell volume calculated with equation 11, and the measured temperatures at which conversion to a single phase was observed. A critical temperature of (838±2) K and a corresponding critical density of (285±10) $kg \cdot m^{-3}$ were derived graphically for 2-aminobiphenyl with these results, as seen in figure 3. Results of measurements on benzene and decane performed as "proof-of-concept measurements" for these procedures have been reported.[28] The rapid heating method was used previously for critical temperature and critical density determinations for dibenzothiophene.[38]

Simultaneous Fit of Vapor-pressure and Two-phase Heat-capacity Results. The critical pressure for 2-aminobiphenyl was not measured directly, but was estimated by means of simultaneous non-linear least-squares fits using the vapor pressures listed in table 4 and the $C^{II}_{x,m}$ values given in table 11. $C_{sat,m}$ values were derived using results of the fit and equation (13). Experimental $C^{II}_{x,m}$ were converted to $C^{II}_{V,m}$ values by means of equation (11) for the cell expansion and the vapor-pressure fit described below for $(\delta p/\delta T)_{sat}$. The values of $C^{II}_{V,m}$ were used to derive functions for $(\delta^2 p/\delta T^2)_{sat}$ and $(\delta^2 \mu/\delta T^2)_{sat}$. The Cox equation[32] was used to represent the vapor pressures in the form:

$$\ln(p/p_C) = (1 - 1/T_r) \exp (A + BT_r + CT_r^2), \quad (14)$$

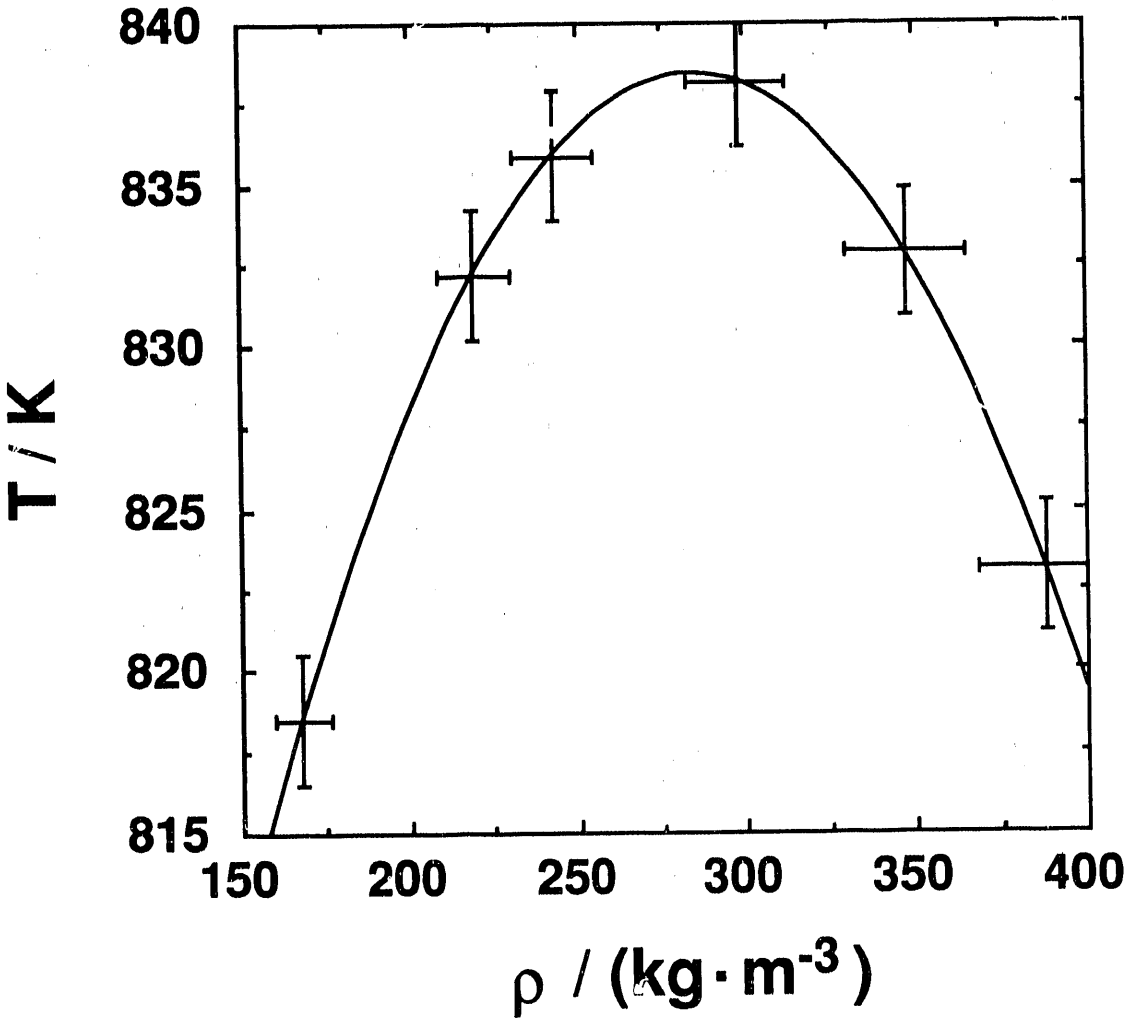

Figure 3. Vapor-liquid coexistence region for 2-aminobiphenyl. The crosses span the range of uncertainty.

with $T_r=T/T_c$, where T_c and p_c are the critical temperature and critical pressure. The critical pressure was included as a variable in the non-linear least-squares analysis. The functional form chosen for variation of the second derivative of the chemical potential with temperature was:

$$(\delta^2\mu/\delta T^2)_{sat} = \sum_{i=0}^{n} b_i(1 - T/T_c)^i. \qquad (15)$$

[For compounds where sufficient information was available to evaluate reliably $(\delta^2\mu/\delta T^2)_{sat}$ (e.g., benzene[39]), four terms (i.e, expansion to n=3) were required to represent the function. Thus, four terms were used in this research.] In these fits the sum of the weighted squares in the following function was minimized:

$$\Delta = C^{II}_{V,m}/R - \{V_m(l)T/nR\}(\delta^2 p/\delta T^2)_{sat} + (T/R)(\delta^2\mu/\delta T^2)_{sat}. \qquad (16)$$

For the vapor-pressure fits, the functional forms of the weighting factors used have been reported.[27] Within the heat-capacity results, the weighting factors were proportional to the square of the mass of sample used in the measurements. Table 13 lists the coefficients determined in the non-linear least-squares fit. A weighting factor of 20 was used to increase the relative weights of the vapor-pressure measurements in the fit. The weighting factor reflects the higher precision of the vapor-pressure values relative to the experimental heat capacities.

Values of $C_{sat,m}$ for 2-aminobiphenyl were derived from $C^{II}_{V,m}(\rho=\rho_{sat})$ with the densities obtained from the corresponding-states equation in the form:[34]

$$(\rho/\rho_c) = 1.0 + 0.85\{1.0 - (T/T_c)\} + (1.692 + 0.986\omega)\{1.0 - (T/T_c)\}^{1/3}, \qquad (17)$$

with $\rho_c = 285\ kg\cdot m^{-3}$, $T_c = 838$ K, and the acentric factor $\omega = 0.456$. The acentric factor is defined as $\{-\lg(p/p_c) - 1\}$, where p is the vapor pressure at $T_r = 0.7$ and p_c is the critical pressure. The Cox equation coefficients given in table 13 were used to calculate p. The results for $C^{II}_{V,m}(\rho = \rho_{sat})/R$ and $C_{sat,m}/R$ are reported in table 14. The estimated uncertainty in these values is 1 per cent.

THERMODYNAMIC PROPERTIES IN THE CONDENSED STATE

Condensed-phase entropies and enthalpies relative to that of the crystals at $T\rightarrow 0$ for the solid and liquid phases under vapor saturation pressure are listed in table 10. These were derived by integration of the smoothed heat capacities corrected for pre-melting, together with the entropies and enthalpies of transition and fusion. The heat capacities

were smoothed with cubic-spline functions by least-squares fits to six points at a time and by requiring continuity in value, slope, and curvature at the junction of successive cubic functions. Due to limitations in the spline-function procedure, some acceptable values from tables 9 and 14 were not included in the fit, while in other regions graphical values were introduced to ensure that the second derivative of the heat capacity with respect to temperature was a smooth function of temperature. Pre-melting corrections were made using standard methods for solid-insoluble impurities and the mole-fraction impurities value shown in table 1.

THERMODYNAMIC PROPERTIES IN THE IDEAL-GAS STATE

Enthalpies and entropies at selected temperatures for the ideal gas were calculated using values in tables 6 and 10 and are listed in columns 2 and 4 of table 15. The derived ideal-gas enthalpies and entropies were combined with the condensed-phase enthalpy of formation given in table 3 to calculate the enthalpies, entropies, and Gibbs energies of formation listed in columns 6, 7, and 8, respectively, of table 15. Enthalpies and entropies for nitrogen and equilibrium hydrogen were determined from JANAF tables.[40] Values for graphite were determined with the polynomial[41] used to calculate the values from 298.15 K to 6000 K listed in the JANAF tables. All uncertainties in table 15 represent one standard deviation and do not include uncertainties in the properties of the elements.

4. DISCUSSION

COMPARISON OF RESULTS WITH LITERATURE

The property-measurement results reported here are the first for this important hydrodenitrogenation intermediate. A search of the literature (1907 to July 1990 Chemical Abstracts) failed to locate any previous thermodynamic property measurements on 2-aminobiphenyl, except for a single enthalpy of combustion study,[42] which is of historical interest only.

THERMODYNAMIC EQUILIBRIA

The calculation of thermodynamic equilibria in organic systems has been outlined in previous reports from this research group.[6,17] The methodology can be summarized as follows. For the general reaction:

$$\text{reactant} + n\ H_2 \Leftrightarrow \text{product},$$

the equilibrium constant, K, is approximately:

$$K = [p_{product} / p_{reactant}] \cdot p_{H_2}^{-n}, \qquad (18)$$

and the Gibbs energies of formation, $\Delta_f G^\circ_m$, for reactants and products are directly related to the equilibrium constant through the relations:

$$\Sigma\ \Delta_f G^\circ_m(\text{products}) - \Sigma\ \Delta_f G^\circ_m(\text{reactants}) = \Delta_r G^\circ_m = -RT \ln K. \qquad (19)$$

[Thus, the experimental Gibbs energies of formation for nitrogen compounds derived in this and earlier reports in this series provide the means to accurately determine equilibrium constants without performing a single reaction. In a more rigorous treatment, the partial pressures are replaced by fugacities. For the experimental conditions discussed in this report, the difference is not significant.] To explicitly demonstrate the effect of hydrogen pressure on the equilibria, a "pseudo-equilibrium" constant, K', is defined:

$$K' = [p_{product} / p_{reactant}] = K \cdot p_{H_2}^{n}\ , \qquad (20)$$

and with equation (2), K' is related to the Gibbs energy of reaction, $\Delta_r G^\circ_m$:

$$\ln K' = -\Delta_r G^\circ_m / RT + n\ [\ln(p_{H_2}/p^\circ)], \qquad (21)$$

where p° is the standard state pressure used in the thermodynamic calculations (101.325 kPa, 1 atm. in this report). As has been noted in previous reports,[5,6,17] if ln K' is plotted versus 1/T, near linear curves are obtained. This facilitates extrapolation of the experimental values obtained at relatively low temperature into the range of commercial processes.

CROSSOVER TEMPERATURE

In order to give as visual a picture as possible of the use of thermodynamics in process engineering, a new concept was introduced in reference 3: the "crossover temperature." For any hydrogenation reaction with a negative Gibbs energy of reaction (i.e., a possible reaction) a crossover temperature can be defined such that below that temperature the reaction is "kinetically controlled." Below the crossover temperature (in the "kinetic-control region"), equilibrium constants derived from Gibbs energies indicate that the reaction can go to completion, though a catalyst may be required for it to go at a measurable rate. In this region, the rate of reaction will increase as the temperature is increased; roughly doubling every 15° C. *Hence, for optimal efficiency the reaction should be performed at the maximum temperature practical (i.e, near as possible to the crossover temperature).*

Above the crossover temperature, the reaction conditions are in the "thermodynamic-control region." In this region an equilibrium exists between the reactants and the products and **increasing the temperature** further results in a **decrease** in the yield of the products. In the thermodynamic-control region, the presence of a catalyst will hasten the attainment of the equilibrium, but will not change the yield. To change the equilibrium condition, special procedures are required such as continuous removal of a product. In the thermodynamic region, increasing the temperature while maintaining all other conditions the same will result in **less** product formation. A pictorial view of the crossover-temperature concept is given in figure 4. By assuming that the crossover between kinetic and thermodynamic control will occur when the equilibrium constant K' drops below 1,000 (0.1 per cent product formation), a quantitative relationship between crossover temperature and hydrogen pressure can be derived. This method is used in the discussion that follows.

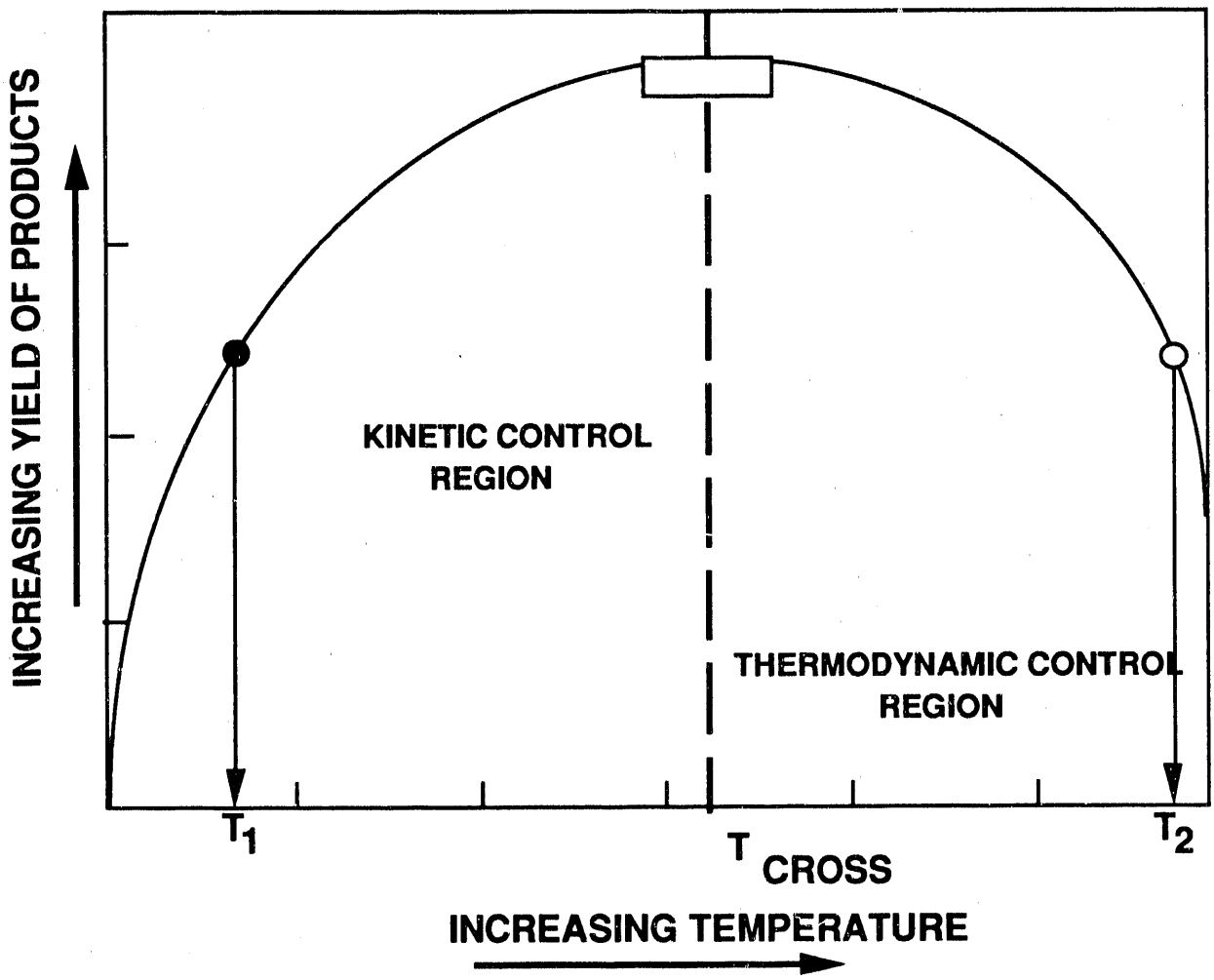

Figure 4. Pictorial view of the crossover-temperature concept. The filled circle denotes the maximum yield of products obtained at temperature T_1: the unfilled circle denotes the maximum yield of products at temperature T_2. (Note the same value for the yield.) Therefore, increasing the temperature can fail to increase the yield since the reaction can change zones from the kinetic-control zone to the thermodynamic-equilibrium-control zone. Maximum process efficiency is obtained within the box on the figure, i.e., near the crossover temperature.

EQUILIBRIA IN DIBENZO SYSTEMS

In the dibenzo systems depicted in figure 5, minimum hydrogen usage requires removal of the central atom of the five-membered ring without hydrogenation of the benzenoid rings. For each of the reactions:

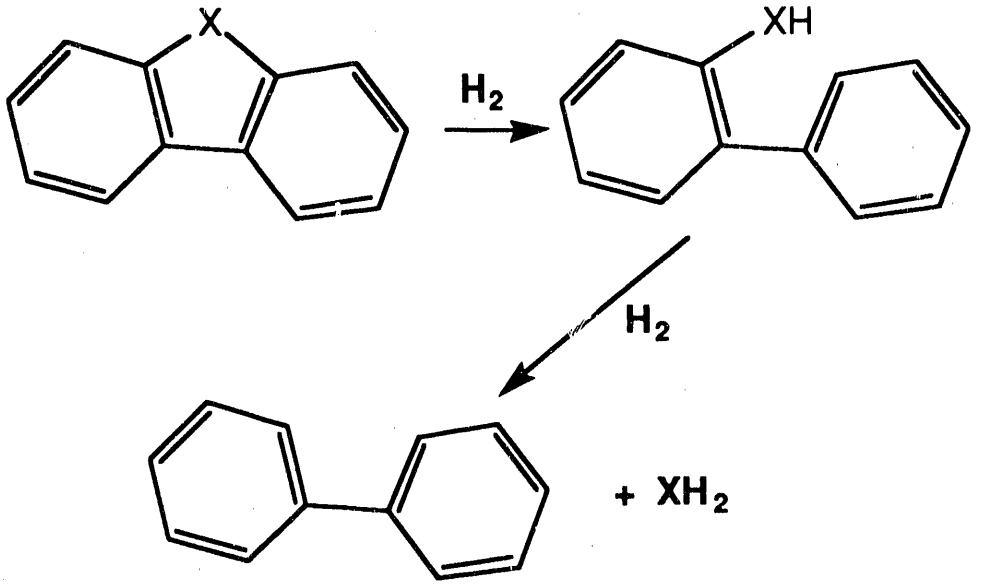

X = CH_2, NH, and O

Figure 5. HDX of dibenzo systems

pseudo-equilibrium constants were derived using equation **21**. Table 16 lists the values for the Gibbs energies of formation for each of the reactants and products (for hydrogen $\Delta_f G^\circ_m$ is zero by definition). Values of $\Delta_r G^\circ_m/RT$ (and hence ln K') were calculated using equation **19** and are listed in table 17. The equations listed in table 18 were derived from plots of ln K' versus 1/T for each reaction.

Crossover-temperature plots for the ring-opening reactions are shown in figure 6. Note that for carbazole and fluorene realistic reaction conditions preclude the ring-opening hydrogenation reaction within the kinetic-control region. For example, the formation of 2-aminobiphenyl from carbazole under kinetic control at 100 atmospheres hydrogen pressure would require a temperature less than –70° C! In contrast, with a suitable catalyst at 100 atmospheres hydrogen pressure, the ring-

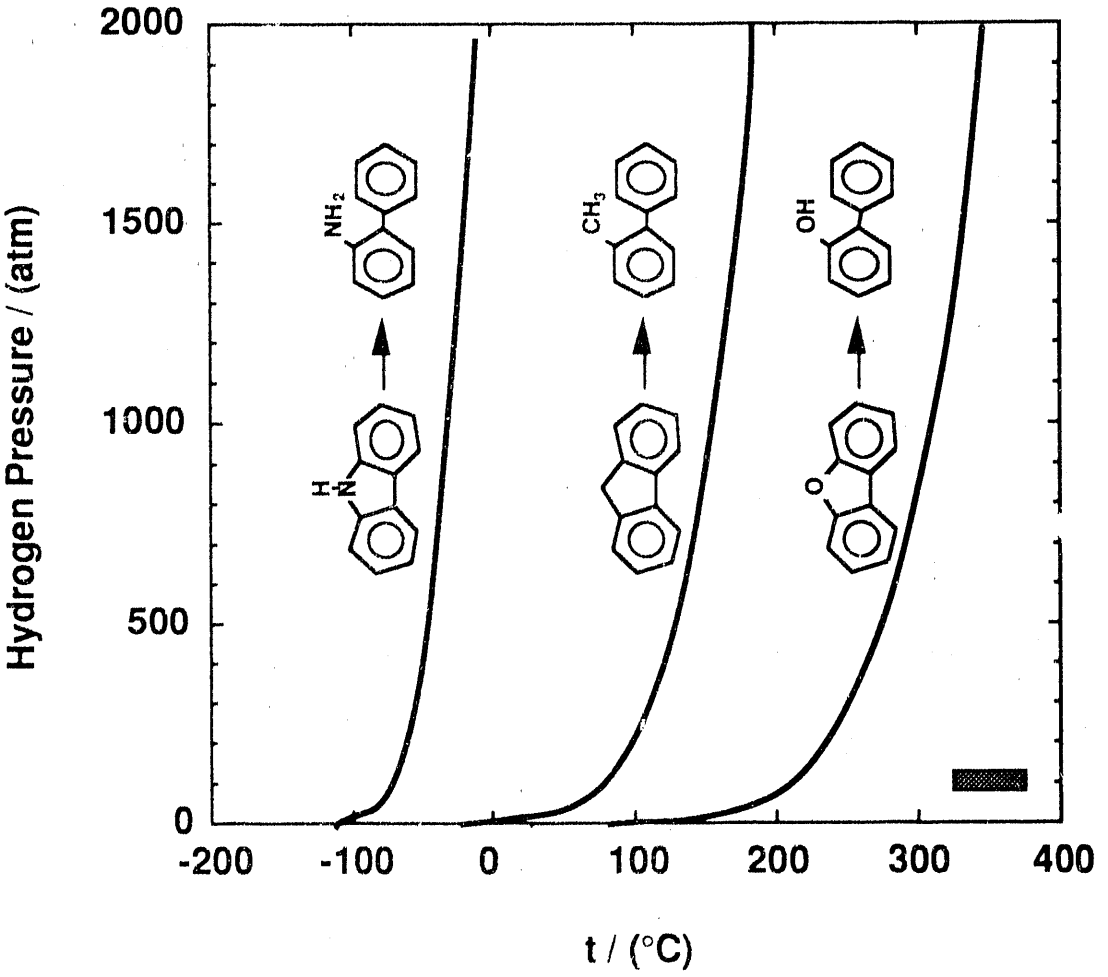

Figure 6. Crossover-temperatures for dibenzo compound ring-opening reactions. Reading from left to right, the curves represent the ring-opening reactions for carbazole, fluorene and dibenzofuran, respectively. For each compound the thermodynamic control region lies to the right of its respective curve. The cross-hatched region represents the range of conventional process conditions.

opening reaction with dibenzofuran could be accomplished in the kinetic-control region provided that the temperature was below 210° C.

Under "conventional" processing conditions (325 to 375° C and 75 to 125 atmospheres hydrogen pressure) all three ring-opening reactions are under thermodynamic control. For carbazole, within the range of conventional processing conditions, thermodynamic calculations (using the equation given in table 18) give between 7 and 15 mole per cent 2-aminobiphenyl under equilibrium conditions. For

fluorene the corresponding calculations give 67 to 86 mole per cent 2-methylbiphenyl under thermodynamic equilibrium. For dibenzofuran the calculations give the range of conversion to 2-hydroxybiphenyl as 96 to 99 mole per cent.

The fate of the 2-substituted biphenyl formed in the initial step of the HDX reaction is important to the overall consumption of hydrogen. Two pathways are possible:

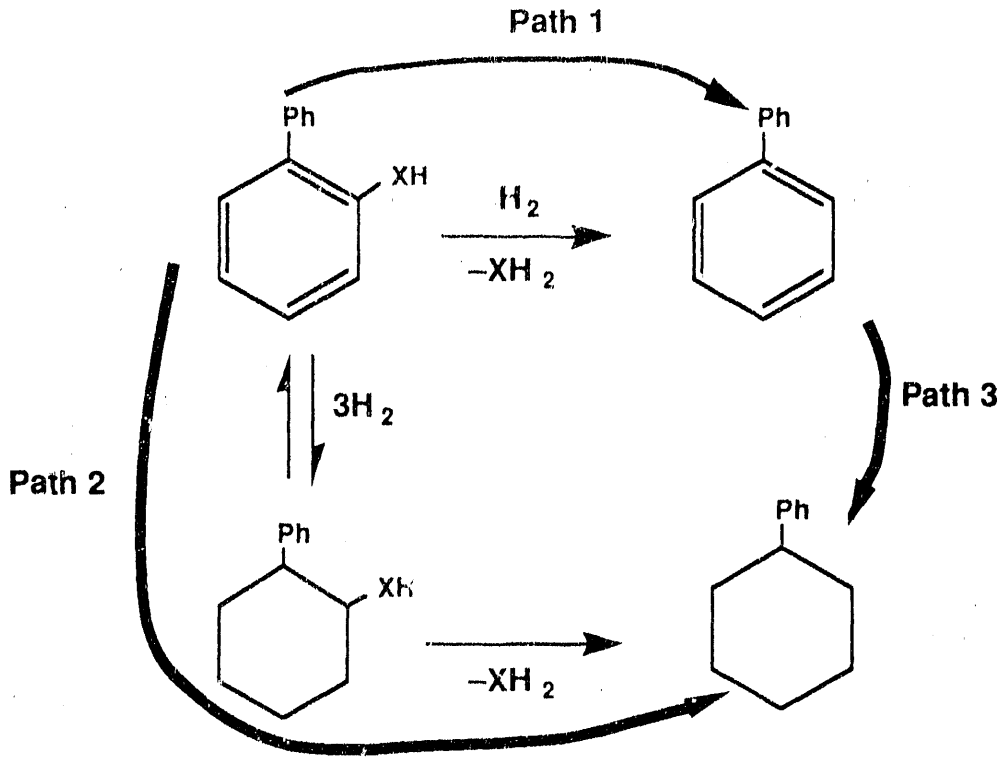

Figure 7. Possible HDX reaction scheme for substituted monoaromatics

Path 1 could continue with subsequent hydrogenation of biphenyl to cyclohexylbenzene (Path 3). However, this is not probable in the carbazole or dibenzofuran cases due to the inhibition of the catalyst surface by the nitrogen- or oxygen-containing compounds present. Such a pathway would be more probable for the HDX of fluorene. For Path 1 thermodynamic calculations, using the equations from table 18, show the reactions to be in the kinetic-control region under all conceivable reaction conditions with hydrogen present. Then the relative reaction rates will be proportional to the strengths of the aromatic-XH bonds. The bond-dissociation energies of Ph-NH_2, Ph-CH_3, and Ph-OH

are listed in reference 43 as 439, 418, and 469 $kJ \cdot mol^{-1}$, respectively. Although the presence of a conventional catalyst will reduce these values somewhat, high temperatures (>300° C) would be required for the reactions to proceed at measurable rates. Hence, Path 2 is the probable route to HDX products.

Under Path 2 the 2-substituted biphenyl is hydrogenated to the corresponding 2-cyclohexyl compound with subsequent H_2X removal. The bond-dissociation energies[4] for cyclohexyl-NH_2, cyclohexyl-CH_3, and cyclohexyl-OH are 351, 356, and 383 $kJ \cdot mol^{-1}$, respectively, and the rates of reaction will be several powers of ten greater than those under Path 1.§ However, in Path 2 the hydrogenation reaction can be within the thermodynamic control region under certain conditions restricting the overall HDX reactions. A detailed discussion of Path 2 would require knowledge of the Gibbs free energies of formation for the substituted cyclohexyl compounds. Research in progress at NIPER (funded by DOE Office of Energy Research) will enable accurate estimation of such values. However, for the carbazole system, an analogy can be found in the quinoline/hydrogen system study published by this group.[6] In the quinoline study, the fate of 2-propylaniline in the HDN reaction scheme parallels that of 2-aminobiphenyl here. The earlier report concluded that at high temperatures (>300° C) the hydrogenation was under thermodynamic control, but propylcyclohexane was the ultimate product due to the fast removal of the hydrogenation product, 2-propylcyclohexylamine. The effect of the lower C-N bond-dissociation energy in the saturated molecule is seen clearly.

As detailed in reference 3 for the quinoline/hydrogen system, zero-valent catalysts may fulfill the requirements needed for the HDX reaction to follow Path 1. Either the Mo/C catalyst used by Skala et al.[44] in HDN reactions or the Re/C in tetralin catalyst under low hydrogen pressure (<5 atmospheres H_2) used by Shaw[45] - again in a HDN study - should result in increased biphenyl selectivity.

COMPARISON WITH LITERATURE HDX STUDIES (X=NH,O,CH_2)

(a) HYDRODENITROGENATION (HDN) OF CARBAZOLE

Due to experimental difficulties (e.g., the high melting point, 521 K; and low solubility in hydrocarbon solvents) there have been relatively few HDN model compound studies on carbazole reported in the literature. Stern[46] reported reaction networks for a range of nitrogen-containing heterocyclic compounds including carbazole. His studies used

---

§ Rate of reaction = $A\, e^{-Ea/RT}$: assuming A factors to be the same via Path 1 or Path 2 the relative rates of reaction will be proportional to the difference in bond-dissociation energies. Using that assumption calculated factors are 10^7, 10^5, and 10^7, respectively.

four different presulfided catalysts ($CoMo/Al_2O_3$, $NiMo/Al_2O_3$, Re/Al_2O_3, and $CoRe/Al_2O_3$) at 350° C and 70 atmospheres hydrogen pressure. 1,2,3,4-Tetrahydrocarbazole was the prime product obtained during the time the reaction was followed with only minor amounts of biphenyl and cyclohexylbenzene observed. Sarbak[47] studied the HDN reaction using presulfided $CoMo/Al_2O_3$, and NiW/Al_2O_3, at 367° C/36 atmospheres hydrogen pressure listing bicyclohexyl as the major product with little biphenyl formed and no cyclohexylbenzene.

Nagai et al.[48-50] have reported results from studies on the HDN reaction of carbazole, carbazole + acridine, and carbazole + various sulfur-containing compounds. The studies used reduced and sulfided Mo/Al_2O_3 catalysts within a wide temperature and pressure regime (260 to 360° C, 45 to 125 atmospheres hydrogen pressure). Neither biphenyl nor cyclohexylbenzene was a major product of the HDN reaction in these studies. The reaction pathway observed was via 1,2,3,4-tetrahydrocarbazole and perhydrocarbazole to produce fully saturated naphthenes as the products (i.e., complete saturation of the aromatic structures).

Yeh[51] studied the HDN reactions of both carbazole and 9-ethylcarbazole using presulfided $CoMo/Al_2O_3$, and $NiMo/Al_2O_3$, at 320° C/172 atmospheres hydrogen pressure. In agreement with most of the other studies, Yeh failed to report biphenyl or cyclohexylbenzene as a reaction product for either compound.

The HDN model compound studies on carbazole reported in the literature illustrate the failure of "conventional" catalysts to make the reaction scheme follow the pathway of minimum or even partial hydrogenation (i.e., 2-aminobiphenyl → biphenyl or 2-aminobiphenyl → 2-phenylcyclohexylamine → cyclohexylbenzene). This is in agreement with the thermodynamic equilibria analysis for the system. Whereas the pathway with the formation of biphenyl is probably impossible, the pathway to cyclohexylbenzene may be attainable with a different catalyst (e.g., a zero-valent catalyst, as discussed in a previous report.[6])

(b) HYDROCRACKING OF FLUORENE

Salim and Bell[52] studied the hydrogenation and cracking of fused three-ring aromatic and hydroaromatic structures present in the liquefaction of coal. The research used $ZnCl_2$ and $AlCl_3$ Lewis acid catalysts under 110 atmospheres hydrogen pressure at 325° C. For fluorene, no reaction was detected using the $ZnCl_2$ catalyst. With $AlCl_3$ the central ring in fluorene was cracked without prior hydrogenation of the aromatic rings producing both diphenylmethane and 2-methylbiphenyl as initial reaction products. The

2-methylbiphenyl formed participated in subsequent reaction-cleavage of the phenyl-phenyl linkage, disproportionation, or both.

Constant et al.[53] hydrocracked fluorene over a nickel-loaded Y zeolite in a fixed-bed flow reactor using decalin as a donor solvent at 388° C and 14.6 atmospheres hydrogen pressure. The central ring in fluorene was cracked without prior hydrogenation of the aromatic rings, producing both diphenylmethane and 2-methyl-biphenyl as initial reaction products. In addition side-ring cracking led to the forming of indans in the reaction products.

The results of the fluorene hydrocracking studies are in agreement with the thermodynamic equilibria analysis given above. Comparison of the diphenylmethane and 2-methylbiphenyl pathways would require Gibbs energies of formation for both compounds. Only partial thermodynamic-property measurements have been reported in the literature for diphenylmethane[54,55] and its properties cannot be estimated using group-additivity methods due to the presence of the "unique" group $C-(C_b)_2(H)_2$.

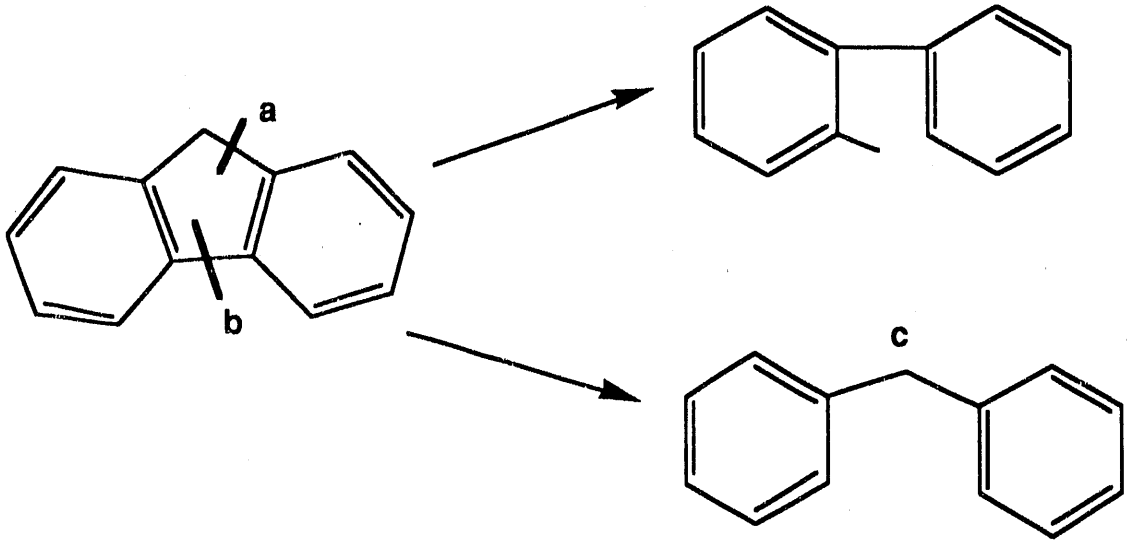

Figure 8. Hydrocracking of fluorene. Breaking bond **a** gives 2-methylbiphenyl. Breaking bond **b** gives diphenylmethane. The "unique" group $C-(C_b)_2(H)_2$ is denoted by **c**.

(c) HYDRODEOXYGENATION (HDO) OF DIBENZOFURAN

Two exhaustive studies on the HDO of dibenzofuran and several possible reaction intermediates have been reported in the literature.[56,57] Krishnamurthy et al.[56] used a batch autoclave at 343 to 376° C and hydrogen pressures 69 to 138 atmospheres

and a presulfided $NiMo/Al_2O_3$ catalyst with CS_2 added to maintain a H_2S pressure during reaction. They also reported on the catalytic HDO of 2-hydroxybiphenyl and 2-cyclohexylphenol. LaVopa and Satterfield[57] studied the hydrodeoxygenation of dibenzofuran, 2-hydroxybiphenyl, 2-cyclohexylphenol, trans-2-phenylcyclohexanol, 2-cyclohexylcylohexanol, and 1,2,3,4-tetrahydrodibenzofuran. The reactions were studied in the temperature range 350 to 390° C at 70 atmospheres hydrogen pressure on a presulfided $NiMo/Al_2O_3$ catalyst. In addition some experiments were performed using the $NiMo/Al_2O_3$ catalyst in the oxidized form with decan-1-ol added to maintain an additional 0.25 atmosphere water pressure in the system.

Both HDO studies are in general agreement except that LaVopa and Satterfield[57] question the identification of 6-phenylhexan-1-ol as a reaction product in the earlier study by Krishnamurthy et al.[56] LaVopa and Satterfield assign the compound as "cyclopentylmethylbenzene" stating that, "A phenylcyclohexanol might plausibly be formed, but if so, it would be expected to be very reactive and unlikely to survive." Further discussion will center on the results of LaVopa and Satterfield.

On both the sulfided and the oxidized forms of the catalyst, LaVopa and Satterfield reported two pathways operating in the HDO of dibenzofuran: (1) hydrogenation of dibenzofuran to hexahydrodibenzofuran, which reacts via 2-cyclohexylphenol to form single-ring hydrocarbons; and (2) direct hydrogenolysis via 2-hydroxybiphenyl, without prior ring hydrogenation, to form biphenyl and cyclohexylbenzene. On the sulfided catalyst, selectivity for single-ring hydrocarbon formation was high; >71 per cent. However, on the catalyst in the oxide form, the selectivity was reversed and 2-ring compounds (biphenyl and cyclohexylbenzene) comprised >75 per cent of the products. The oxide form of the catalyst was less active than the sulfided form. The per cent of HDO at 360° C, 70 atmospheres hydrogen pressure with 0.25 atmospheres H_2O present was only 19 per cent compared to 55 per cent on the sulfided catalyst with 0.07 atmospheres H_2S present.

LaVopa and Satterfield[57] reported that 2-hydroxybiphenyl reacts to form biphenyl and cyclohexylbenzene. Although both biphenyl and cyclohexylbenzene underwent secondary hydrogenation, the hydrogenation of biphenyl alone proceeded much slower (a factor of 4 times slower) than the HDO of 2-hydroxybiphenyl. They calculated that if the cyclohexylbenzene was formed only through biphenyl hydrogenation, the concentration of biphenyl would have reached a maximum value of 61 per cent of the initial concentration of 2-hydroxybiphenyl rather than the 10 per cent observed.

The results of the HDO studies of LaVopa and Satterfield are in agreement with the thermodynamic equilibria analysis given above. For the HDO of 2-hydroxybiphenyl, the studies highlight the presence of two competing pathways (Path 1 and Path 2 in

figure 7) leading to biphenyl and cyclohexylbenzene as reaction products. LaVopa and Satterfield also showed the improbability of the reaction following Path 3; i.e., biphenyl to cyclohexylbenzene. In the competition between Path 1 and Path 2, the latter is favored by a factor of 6 using the presulfided $NiMo/Al_2O_3$ catalyst. For the HDO of dibenzofuran, the reaction pathway depicted in figure 7 occurs using both forms of catalyst. If minimization of hydrogen consumption is the goal of hydroprocessing of liquids containing compounds with dibenzofuran moieties present, then the oxide form of the catalyst obviously is preferred. However, the presence of sulfur compounds in the processing liquid will restrict the operation of such a catalyst. The same problem was noted in NIPER-468[6] when the HDN of quinoline was discussed.

5. SUMMARY and HIGHLIGHTS

- Thermochemical and thermophysical properties for 2-aminobiphenyl are reported. The properties measured included the energy of combustion, and vapor pressures and heat capacities over a range of temperatures. Gibbs energies of formation for equilibria calculations were derived.

- Values for the critical properties of 2-aminobiphenyl were determined. The results, which illustrate the inherent thermal stability of the amine, are the first such experimental measurements reported for a 2-substituted biphenyl.

- Ideal-gas thermodynamic properties for 2-aminobiphenyl were determined based on the accurate calorimetric measurements. No previous calorimetric measurements on this important hydrodenitrogenation intermediate have been reported in the literature.

- Thermodynamic equilibria calculations were made on the carbazole/2-aminobiphenyl/hydrogen system and the results compared with those for the fluorene/2-methylbiphenyl/hydrogen and the dibenzofuran/2-hydroxybiphenyl/hydrogen systems. The results give the following reactivity order for the ring-opening (hydrogenolysis) reaction:

  carbazole < fluorene < dibenzofuran.

- The thermodynamic equilibria results are confirmed by batch-reaction studies reported in the literature. For the hydrodenitrogenation of carbazole, the reaction pathway using the minimum of hydrogen (carbazole → 2-aminobiphenyl → biphenyl) probably cannot be realized but the pathway (carbazole →

2-aminobiphenyl → 2-phenylcyclohexylamine → cyclohexylbenzene) should be possible with proper catalyst selection. The literature results confirm the minimum hydrogen pathway for fluorene. For dibenzofuran, the literature results confirm the possibility of the minimum hydrogen usage pathway using an oxide based catalyst. On an oxide catalyst the selectivity for 2-ring products (biphenyl and cyclohexylbenzene) was >75 per cent.

- If minimization of hydrogen consumption is the goal of hydroprocessing of liquids containing compounds with carbazole and/or dibenzofuran moieties present, then catalysts other than those used in present refineries will be required. However, as was noted in our previous topical report on the hydrodenitrogenation of quinoline, the presence of sulfur compounds in the processing liquid will restrict the operation of such a catalyst. Upgrading of such liquids will require new processing technology such as "Staged Upgrading." Staged Upgrading, as used in this context, is where different compound types are removed under conditions which favor their individual removal. For example, sulfur compounds are removed first followed by nitrogen compounds under a completely different set of conditions of catalyst, hydrogen pressure and temperature. This concept will be the subject of a future topical report from this group.

6. REFERENCES

1. Steele, W. V.; Chirico, R. D.; Collier, W. B.; Harrison, R. H.; Gammon, B. E. *Assessment of Thermodynamic Data and Needs, Including Their Economic Impact, for Development of New Fossil Fuel Refining Processes.* NIPER-159. Published by DOE Fossil Energy, Bartlesville Project Office. Available from NTIS Report No. DE-86000298, June **1986.**
2. Katzer, J. R.; Sivasubramanian, R. *Catal. Rev.-Sci. Eng.* **1979**, 20, 155.
3. Ledorix, M. *J. Catalysis (London)* **1985,** 7, 125.
4. Ho, T. C. *Catal. Rev.-Sci. Eng.* **1988**, 30, 117.
5. Steele, W. V., and R. D. Chirico. *Thermodynamics and the Hydrodenitrogenation of Indole. In three parts: Part I. Thermodynamic Properties of Indoline and 2-Methylindole, Part II. Gibbs Energies of Reaction in the Hydrodenitrogenation of Indole, Part III. Thermodynamic Equilibria and Comparison with Literature Kinetic Studies.* NIPER-415. Published by DOE Fossil Energy, Bartlesville Project Office. Available from NTIS, Report No. DE-89000751, June **1989.**
6. Steele, W. V.; Chirico, R. D. *Thermodynamics of the Hydrodenitrogenation of Quinoline.* NIPER-468. Published by DOE Fossil Energy, Bartlesville Project Office. Available from NTIS Report No. DE-90000245, June **1990.**
7. Commission on Atomic Weights and Isotopic Abundances. *Pure Appl. Chem.* **1983**, 55, 1101.
8. Cohen, E. R.; Taylor, B. N. *J. Phys. Chem. Ref. Data* **1988**, 17, 1795.
9. *Metrologia* **1969**, 5, 35.
10. McCrackin, F. L.; Chang, S. S. *Rev. Sci. Instrum.* **1975**, 46, 550.
11. Good, W. D.; Moore, R. T. *J. Chem. Eng. Data* **1970**, 15, 150.
12. Good, W. D.; Smith, N. K. *J. Chem. Eng. Data* **1969,** 14, 102.
13. Good, W. D. *J. Chem. Eng. Data* **1969,** 14, 231.
14. Good, W. D.; Scott, D. W.; Waddington, G. *J. Phys. Chem.* **1956,** 60, 1080.
15. Good, W. D.; Douslin, D. R.; Scott, D. W.; George, A.; Lacina, J. L.; McCullough, J. P.; Waddington, G. *J. Phys. Chem.* **1959**, 63, 1133.
16. Smith, N. K.; Stewart, R. C., Jr.; Osborn, A. G.; Scott, D. W. *J. Chem. Thermodynamics* **1980,** 12, 919.
17. Chirico, R. D.; Hossenlopp, I. A.; Nguyen, A.; Strube, M. M.; Steele, W. V. *Thermodynamic Studies Related to the Hydrogenation of Phenanthrene.* NIPER-247. Published by DOE Fossil Energy, Bartlesville Project Office. Available from NTIS Report No. DE-87001252, April **1987.**

18. Goldberg, R. N.; Nuttall, R. N.; Prosen, E. J.; Brunetti, A. P. *NBS Report 10437,* U. S. Department of Commerce, National Bureau of Standards, June **1971**.
19. Hubbard, W. N.; Scott, D. W.; Waddington, G. *Experimental Thermochemistry.* Rossini, F. D.: editor. Interscience: New York, **1956**, Chapt. 5, pp. 75-128.
20. Smith, N. K.; Good, W. D. *J. Chem. Eng. Data* **1967,** 12, 572.
21. Swietoslawski, W. *Ebulliometric Measurements.* Reinhold: New York, **1945**.
22. Osborn A. G.; Douslin, D. R. *J. Chem. Eng. Data* **1966,** 11, 502.
23. Chirico, R. D.; Nguyen, A.; Steele, W. V.; Strube, M. M.; Tsonopoulos, C. *J. Chem. Eng. Data* **1989**, 34, 149.
24. Antoine, C. *C. R. Acad. Sci.* **1888**, 107, 681.
25. Douslin, D. R.; McCullough, J. P. *U. S. Bureau of Mines. Report of Investigation 6149*, **1963**, pp. 11.
26. Douslin, D. R.; Osborn A. G. *J. Sci. Instrum.* **1965**, 42, 369.
27. Steele, W. V.; Archer, D. G.; Chirico, R. D.; Collier, W. B.; Hossenlopp, I. A.; Nguyen, A.; Smith, N. K.; Gammon, B. E. *J. Chem. Thermodynamics* **1988,** 20, 1233.
28. Steele, W. V.; Chirico, R. D.; Knipmeyer, S. E.; Smith, N. K. *High-Temperature Heat-Capacity Measurements and Critical Property Determinations using a Differential Scanning Calorimeter. (Development of Methodology and Application to Pure Organic Compounds)* NIPER-360, December **1988**. Published by DOE Fossil Energy, Bartlesville Project Office. Available from NTIS Order No. DE89000709.
29. Rossini, F. D. *Experimental Thermochemistry.* Rossini, F. D.: editor. Interscience: New York. **1956**, Chapt. 14, pp. 297-320.
30. Cox, J. D.; Wagman, D. D.; Medvedev, V. A.: editors. *CODATA Key Values for Thermodynamics.* Hemisphere: New York. **1989**.
31. Scott, D. W.; Osborn, A. G. *J. Phys. Chem.* **1979**, 83, 2714.
32. Cox, E. R. *Ind. Eng. Chem.* **1936**, . 613.
33. Pitzer, K. S.; Curl, R. F. Jr. *J. Am. Chem. Soc.* **1957**, 79, 2369.
34. Hales, J. L.; Townsend, R. *J. Chem. Thermodynamics* **1972**, 4, 763.
35. Orbey, H.; Vera, J. H. *AIChE Journal*, **1983**, 29, 107.
36. Steele, W. V.; Chirico, R. D. To be submitted to *Ind. Eng. Res.*
37. McCullough, J. P.; Waddington, G. *Anal. Chim. Acta* **1957**, 17, 80.
38. Chirico, R. D.; Knipmeyer, S. E.; Nguyen, A.; Steele, W. V. Submitted to *J. Chem. Thermodynamics* **1990**.
39. Goodwin, R. D. *J. Phys. Chem. Ref. Data* **1988**, 17, 1541.

40. Chase, M. W., Jr.; Davies, C. A.; Cowney, J. R.; Frurip, D. J.; McDonald, R. A.; Syverud, A. N. *JANAF Thermochemical Tables* Third edition. Supplement to *J. Phys. Chem. Ref. Data* **1985**, 14.
41. Chirico, R. D.; Archer, D. G.; Hossenlopp, I. A.; Nguyen, A.; Steele, W. V.; Gammon, B. E. *J. Chem. Thermodynamics* **1990**, 22, 665.
42. Brull, L. *Gazz. Chim. Ital.* **1935**, 65, 19.
43. Benson, S. W. *Thermochemical Kinetics.* 2nd edition. Wiley: New York, **1976**.
44. Skala, D. U., Saban, M. D.; Jovanovic, J. A.; Meyn, V. W.; Rahimian, I. G-H. *Ind Eng. Chem. Res.* **1988**, 27, 1186.
45. Shaw, J. E. *Fuel* **1988**, 67, 1706.
46. Stern, E. W. *J. Catalysis* **1975**, 57, 380.
47. Sarbak, Z. *React. Kinet. Catal. Lett.* **1986**, 32, 435.
48. Nagai, M.; Sawahiraki, K.; Kabe, T. *Nippon Kagaka Kaishi* **1980**, p. 69.
49. Nagai, M.; Masunaga, T. *Fuel* **1988**, 67, 771.
50. Nagai, M.; Masunaga, T; Hana-oka, N. *Energy & Fuels* **1988**, 2, 645.
51. Yeh, Ji-C. *Hydrodenitrogenation Studies of Condensed Carbocyclic-N-Heterocyclic Compounds and of an SRC-II Distillate* PhD Thesis. University of Utah. March **1985**.
52. Salim, S. S.; Bell, A. T. *Fuel* **1984**, 63, 469.
53. Constant, W. D.; Price, G. L.; McLaughlin, E. *Fuel* **1986**, 65, 8.
54. Huffman, H. M.; Parks, G. S.; Daniels, A. C. *J. Am. Chem. Soc.* **1930**, 52, 1547.
55. Smith, R. H.; Andrews, D. H. *J. Am. Chem. Soc.* **1931**, 53, 3644.
56. Krishnamurthy, S.; Panvelker, S.; Shah, Y. T. *AIChE J.* **1981**, 27, 994.
57. LaVopa, V.; Satterfield, C. N. *Energy & Fuels* **1987**, 1, 323.

TABLE 1. Calorimeter and sample characteristics: m is the sample mass; V_i is the internal volume of the calorimeter; T_{cal} is the temperature of the calorimeter when sealed; p_{cal} is the pressure of the helium and sample when sealed; r is the ratio of the heat capacity of the full calorimeter to that of the empty; T_{max} is the highest temperature of the measurements; and $\delta C/C$ is the vaporization correction; x_{pre} is the mole-fraction impurity used for pre-melting corrections.

2-Aminobiphenyl

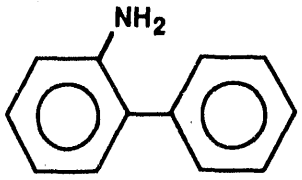

m/g	52.976
V_i(298.15 K)/cm^3	62.47
T_{cal}/K	298.7
p_{cal}/kPa	5.33
r(T_{max})	3.8
r_{min}	2.0
$10^2(\delta C/C)_{max}$	0.002
x_{pre}	0.0002

TABLE 2 Typical combustion experiment for 2-aminobiphenyl at 298.15 K. (p° = 101.325 kPa) [a]

m'(compound)/g	0.900718
m"(fuse)/g	0.00563
$n_i(H_2O)$/mol	0.05535
m(Pt)/g	20.806
$\Delta T=(t_i - t_f + \Delta t_{corr})$/K	2.02894
ε(calor)(ΔT)/J	−34026.7
ε(cont)(ΔT)/J [b]	−37.2
ΔU_{ign}/J	0.75
$\Delta U_{dec}(HNO_3)$/J	48.9
ΔU(corr. to std. states)/J [c]	19.6
$-m''(\Delta_c U^\circ_m/M)$(fuse)/J	26.5
$m'(\Delta_c U^\circ_m/M)$(compound)/J	−33968.1
$(\Delta_c U^\circ_m/M)$(compound)/J·g^{-1}	−37712.2

[a] The symbols and abbreviations of this table are those of reference 19 except as noted.

[b] $\varepsilon_i(cont)(t_i - 298.15\ K) + \varepsilon_f(cont)(298.15\ K - t_f + \Delta t_{corr})$

[c] Items 81 to 85, 87 to 90, 93, and 94 of the computational form of reference 19.

TABLE 3. Summary of experimental energies of combustion and molar thermochemical functions for 2-aminobiphenyl at T = 298.15 K and p° = 101.325 kPa.

$\{(\Delta_c U^\circ_m/M)(\text{compound})\}/(J\cdot g^{-1})$					
−37712.2	−37715.8	−37713.8	−37717.7	−37718.1	−37712.8

$\langle\{(\Delta_c U^\circ_m/M)(\text{compound})\}/(J\cdot g^{-1})\rangle$	−37715.0±1.0
$(\Delta_c U^\circ_m)(\text{compound})/(kJ\cdot mol^{-1})$	−6382.39±0.88
$(\Delta_c H^\circ_m/M)(\text{compound})/(kJ\cdot mol^{-1})$	−6387.97±0.88
$(\Delta_f H^\circ_m/M)(\text{compound})/(kJ\cdot mol^{-1})$	93.79±1.06

TABLE 4. Summary of vapor-pressure results for 2-aminobiphenyl: IP refers to measurements performed with the inclined-piston gauge; water or decane refers to which material was used as the standard in the reference ebulliometer; T is the temperature of the experimental inclined-piston pressure gauge measurements or, for ebulliometric measurements, of the condensation temperature of the sample; the pressure p for ebulliometric measurements was calculated from the condensation temperature of the reference substance; Δp is the difference of the calculated value of pressure from the observed value of pressure; σ_i is the propagated error calculated from equations (1) and (2); ΔT is the difference between the boiling and condensation temperatures ($T_{boil} - T_{cond}$) for the sample in the ebulliometer.

Method	$\frac{T}{K}$	$\frac{p}{kPa}$	$\frac{\Delta p}{kPa}$	$\frac{\sigma_i}{kPa}$	$\frac{\Delta T}{K}$
IP	350.000 [a]	0.0165	−0.0001	0.0002	
IP	350.001 [a]	0.0169	0.0004	0.0002	
IP	350.000	0.0167	0.0001	0.0002	
IP	360.002 [a]	0.0336	0.0004	0.0002	
IP	360.000	0.0334	0.0002	0.0002	
IP	370.002 [a]	0.0632	−0.0003	0.0002	
IP	369.998	0.0635	0.0000	0.0002	
IP	379.999	0.1165	0.0001	0.0002	
IP	389.999	0.2058	0.0004	0.0002	
IP	399.999	0.3503	0.0005	0.0003	
IP	410.003	0.5775	0.0005	0.0003	
IP	419.999	0.9238	0.0006	0.0003	
IP	430.001	1.4382	0.0005	0.0004	
decane	437.854	2.0000	0.0004	0.0001	0.143
IP	440.002	2.1828	0.0001	0.0005	
IP	445.001	2.6651	−0.0003	0.0006	
decane	445.010	2.6660	−0.0003	0.0002	0.112
IP	450.003	3.2366	−0.0004	0.0007	
decane	455.621	3.9999	−0.0006	0.0002	0.068
decane	463.541	5.3330	−0.0001	0.0003	0.059
decane	475.327	7.9989	0.0000	0.0004	0.051
decane	484.171	10.6661	0.0001	0.0005	0.044

Table 4. Continued

Method	T / K	p / kPa	Δp / kPa	σ| / kPa	ΔT / K
decane	491.327	13.332	−0.002	0.001	0.037
decane	498.752	16.665	0.000	0.001	0.037
decane	504.924	19.933	0.000	0.001	0.034
decane	513.050	25.023	0.000	0.001	0.030
water	513.046 [a]	25.023	0.003	0.001	0.032
water	521.224	31.177	0.005	0.002	0.025
water	529.459	38.565	0.004	0.002	0.023
water	537.749	47.375	0.001	0.002	0.020
water	546.092	57.817	−0.001	0.003	0.013
water	554.486	70.120	0.000	0.003	0.015
water	562.936	84.533	0.001	0.004	0.015
water	571.440	101.325	−0.001	0.004	0.013
water	579.997	120.79	0.00	0.01	0.011
water	588.608	143.25	0.00	0.01	0.012
water	597.268	169.02	0.00	0.01	0.012
water	605.987	198.49	−0.01	0.01	0.013
water	614.748	232.02	0.00	0.01	0.021
water	623.558	270.02	−0.01	0.01	0.028

[a] The value at this temperature was not included in the fit.

TABLE 5. Cox equation coefficients for 2-aminobiphenyl

T_{ref}/K	838
p_{ref}/kPa	3933
A	2.68956
10^3B	−1.98948
10^6C	1.55266
T/K [a]	350 to 623

[a] Temperature range of the vapor pressures used in the fit.

TABLE 6. Enthalpies of vaporization and entropies of compression for 2-aminobiphenyl obtained from the Cox and Clapeyron equations [a]

T/K	$\Delta_l^g H_m/RK$	$\Delta S_{comp,m}/R$	T/K	$\Delta_l^g H_m/RK$	$\Delta S_{comp,m}/R$
298.15 [b]	9427±10	−13.255±0.001	560.00	6635±23	−0.245±0.000
300.00 [b]	9404±10	−13.060±0.001	580.00	6431±30	0.176±0.000
320.00 [b]	9161±7	−11.126±0.001	600.00	6221±38	0.563±0.000
340.00 [b]	8923±5	−9.463±0.000	620.00	6004±48	0.920±0.000
360.00	8692±3	−8.023±0.000	640.00 [b]	5780±59	1.250±0.000
380.00	8467±2	−6.769±0.000	660.00 [b]	5544±71	1.558±0.000
400.00	8248±1	−5.668±0.000	680.00 [b]	5295±84	1.846±0.000
420.00	8036±1	−4.698±0.000	700.00 [b]	5029±99	2.116±0.000
440.00	7829±2	−3.838±0.000	720.00 [b]	4740±116	2.370±0.000
460.00	7627±3	−3.071±0.000	740.00 [b]	4422±134	2.612±0.000
480.00	7428±5	−2.385±0.000	760.00 [b]	4064±154	2.842±0.000
500.00	7231±8	−1.768±0.000	780.00 [b]	3652±176	3.062±0.000
520.00	7034±12	−1.211±0.000	800.00 [b]	3160±201	3.274±0.000
540.00	6836±17	−0.706±0.000	820.00 [b]	2530±230	3.479±0.000

[a] $\Delta S_{comp}/R = \ln(p/p^\circ)$ where $p^\circ = 101.325$ kPa and $R = 8.31451\ J \cdot K^{-1} \cdot mol^{-1}$.

[b] Values at this temperature were calculated with extrapolated vapor pressures determined from the fitted Cox coefficients.

TABLE 7. Melting-study summary for 2-aminobiphenyl: F is the fraction melted at observed temperature T(F); T_{tp} is the triple-point temperature; x is the mole-fraction impurity

F	T(F)/K
0.208	322.206
0.357	322.240
0.506	322.253
0.655	322.259
0.804	322.263
T_{tp}/K	322.28
x	0.00024

TABLE 8. Experimental molar enthalpy measurements for 2-aminobiphenyl
(R=8.31451 $J \cdot K^{-1} \cdot mol^{-1}$)

N [a]	h [b]	$\frac{T_i}{K}$	$\frac{T_f}{K}$	$\frac{T_{trs}}{K}$	$\frac{\Delta_{tot}H_m}{R \cdot K}$ [c]	$\frac{\Delta_{trs}H_m}{R \cdot K}$ [d]
		Single-phase measurements in cr(II)				
10	1	188.455	234.672		867.08	−0.05
13	1	74.725	173.170		1173.46	0.16
13	1	173.492	249.397		1424.81	−0.87
		cr(II) to cr(I)				
6	1	255.674	260.736	258.0	116.80	−0.24 [e]
10	1	255.153	265.438		239.74	−0.02
13	1	255.743	264.995		215.84	0.03
					Average:	0.00
		Single-phase measurements in cr(I)				
9	1	275.838	314.919		1034.05	0.95
14	1	284.502	315.068		820.03	0.08
		cr(I) to liquid				
2	6	318.939	324.890	322.28	1874.24	1681.83
8	2	309.523	325.000		2143.86	1682.82
14	2	315.424	324.644		1965.14	1682.21
					Average:	1682.29
		Single-phase measurements in liquid				
16	1	344.817	430.070		3428.83	−0.24

[a] Adiabatic series number

[b] Number of heating increments

[c] $\Delta_{tot}H_m$ is the molar energy input from the initial temperature T_i to the final temperature T_f.

[d] $\Delta_{trs}H_m$ is the net molar enthalpy of transition at the transition temperature T_{trs} or the excess enthalpy relative the heat-capacity curve described in the text for single-phase measurements

[e] This value was not included in the average.

TABLE 9. Experimental molar heat capacities at vapor-saturation pressure for 2-aminobiphenyl ($R = 8.31451\ J \cdot K^{-1} \cdot mol^{-1}$)

N[a]	<T>/K	ΔT/K	$C_{sat,m}/R$[b]	N[a]	<T>/K	ΔT/K	$C_{sat,m}/R$[b]
			cr(II)				
12	5.386	0.7416	0.089	11	83.613	8.1945	8.949
12	6.277	0.9631	0.128	11	92.203	8.9589	9.587
12	7.199	0.9327	0.194	11	101.407	9.4529	10.260
12	8.178	1.0373	0.276	11	111.129	9.9970	10.964
12	9.226	1.0756	0.385	11	121.109	9.9732	11.689
12	10.336	1.1531	0.503	11	131.103	10.0200	12.422
12	11.536	1.2509	0.653	11	141.155	10.0929	13.168
12	12.867	1.3907	0.843	11	151.272	10.1851	13.928
12	14.327	1.4978	1.059	11	161.870	10.2753	14.742
12	15.908	1.6632	1.304	11	172.188	10.3351	15.548
12	17.705	1.9154	1.589	11	182.567	10.4041	16.366
12	19.704	2.0709	1.912	11	192.819	10.0872	17.202
12	21.888	2.2913	2.270	11	203.167	10.5948	18.049
12	24.301	2.5273	2.661	11	213.838	10.6459	18.939
12	26.946	2.7791	3.080	11	224.489	10.6495	19.848
12	29.900	3.1359	3.535	11	235.143	10.6558	20.790
12	33.221	3.4900	4.031	10	239.802	10.1914	21.225
12	36.894	3.8428	4.542	11	244.352	7.7638	21.640
12	40.987	4.3316	5.065	6	244.568	10.0669	21.648
12	45.577	4.8384	5.604	10	247.482	5.1023	21.967
12	50.679	5.3608	6.154	13	252.574	5.6429	22.522
11	51.842	4.5891	6.274	10	252.589	5.0234	22.516
11	56.794	5.2918	6.759	6	252.641	6.0421	22.447
11	62.491	6.0814	7.267	6	258.205	5.0615	23.081
11	68.866	6.6437	7.803	10	260.296	10.2849	23.316
11	75.853	7.3202	8.357	13	260.369	9.2528	23.332

TABLE 9. Continued

N[a]	<T>/K	ΔT/K	$C_{sat,m}$[b]/R	N[a]	<T>/K	ΔT/K	$C_{sat,m}$[b]/R
			cr(l)				
6	264.206	6.9824	23.626	7	284.696	9.9343	25.531
10	268.893	6.8978	24.105	8	292.784	11.0829	26.246
6	270.588	5.8911	24.244	7	294.878	10.1574	26.398
5	273.710	6.2502	24.502	8	304.011	10.8245	27.248
7	275.987	6.7891	24.720	7	305.147	10.1467	27.348
6	278.406	9.8630	24.938	2	307.325	7.2024	27.648
8	281.609	10.8950	25.248	2	315.161	7.1766	28.715
			liquid				
3	295.390	5.3980	35.727	3	338.259	8.8639	37.768
3	302.578	8.9424	36.069	15	344.565	13.2290	38.079
3	311.507	8.8783	36.477	15	358.181	13.9563	38.755
3	320.374	8.8141	36.898	15	372.507	14.6601	39.471
2	328.477	7.1494	37.284	15	387.095	14.4932	40.205
14	329.038	8.7517	37.316	15	401.515	14.3349	40.927
3	329.258	8.9301	37.325	15	415.736	14.1819	41.642
8	329.382	8.7497	37.330	15	429.423	13.2132	42.330
15	332.326	10.6899	37.474	15	440.488	8.9379	42.889
2	335.698	7.1063	37.644				

[a] Adiabatic series number.

[b] Average heat capacity for a temperature increment of ΔT with a mean temperature <T>.

TABLE 10. Molar thermodynamic functions at vapor-saturation pressure for 2-aminobiphenyl ($R = 8.31451\ J \cdot K^{-1} \cdot mol^{-1}$)

$\frac{T}{K}$	$\frac{C_{sat,m}}{R}$	$\frac{\Delta_0^T S_m^o}{R}$	$\frac{\Delta_0^T H_m^o}{RT}$	$\frac{T}{K}$	$\frac{C_{sat,m}}{R}$	$\frac{\Delta_0^T S_m^o}{R}$	$\frac{\Delta_0^T H_m^o}{RT}$
			cr(II)				
5.000	0.066	0.022	0.016	150.000	13.832	14.832	7.665
10.000	0.468	0.169	0.125	160.000	14.597	15.749	8.074
15.000	1.162	0.482	0.349	170.000	15.376	16.657	8.480
20.000	1.960	0.925	0.651	180.000	16.162	17.558	8.885
30.000	3.551	2.025	1.357	190.000	16.971	18.453	9.289
40.000	4.943	3.244	2.085	200.000	17.789	19.345	9.694
50.000	6.084	4.474	2.774	210.000	18.616	20.232	10.099
60.000	7.050	5.671	3.409	220.000	19.460	21.118	10.505
70.000	7.895	6.822	3.990	230.000	20.327	22.002	10.913
80.000	8.676	7.927	4.527	240.000	21.220	22.886	11.324
90.000	9.425	8.993	5.030	245.000	21.705	23.328	11.531
100.000	10.157	10.024	5.506	250.000	22.228	23.772	11.740
110.000	10.882	11.026	5.962	252.000	22.437	23.950	11.824
120.000	11.608	12.004	6.402	254.000	22.645	24.128	11.908
130.000	12.341	12.962	6.831	256.000	22.866	24.307	11.993
140.000	13.081	13.904	7.251	258.000	23.133	24.486	12.078
			cr(I)				
258.000	23.133	24.486	12.078	298.150	26.683	28.081	13.805
260.000	23.305	24.665	12.164	300.000	26.846	28.247	13.885
270.000	24.179	25.561	12.593	310.000	27.724	29.141	14.317
280.000	25.076	26.456	13.022	320.000	28.597	30.035	14.750
290.000	25.964	27.352	13.453	322.280	28.795	30.239	14.849
			liquid				
298.150	35.862	32.625	18.745	500.000	46.101	53.517	27.668
300.000	35.950	32.847	18.851	520.000	47.219	55.347	28.398
310.000	36.409	34.033	19.410	540.000	48.343	57.150	29.116
320.000	36.880	35.197	19.948	560.000	49.463	58.929	29.823
322.280	36.989	35.459	20.069	580.000	50.565	60.684	30.519

TABLE 10. continued

$\frac{T}{K}$	$\frac{C_{sat,m}}{R}$	$\frac{\Delta_0^T S_m^o}{R}$	$\frac{\Delta_0^T H_m^o}{RT}$	$\frac{T}{K}$	$\frac{C_{sat,m}}{R}$	$\frac{\Delta_0^T S_m^o}{R}$	$\frac{\Delta_0^T H_m^o}{RT}$
			liquid (continued)				
330.000	37.362	36.339	20.469	600.000	51.633	62.416	31.205
340.000	37.854	37.462	20.973	620.000	52.650	64.126	31.880
350.000	38.348	38.566	21.462	640.000	53.600	65.813	32.545
360.000	38.846	39.653	21.938	660.000	54.467	67.475	33.196
370.000	39.346	40.724	22.402	680.000	55.239	69.113	33.833
380.000	39.848	41.780	22.854	700.000	55.914	70.724	34.455
390.000	40.350	42.822	23.297	720.000	56.501	72.308	35.059
400.000	40.851	43.850	23.729	740.000	57.038	73.863	35.646
420.000	41.856	45.867	24.568	760.000	57.622	75.392	36.216
440.000	42.865	47.838	25.377	780.000	58.476	76.898	36.775
460.000	43.918	49.766	26.160	800.000	60.275	78.398	37.337
480.000	44.999	51.658	26.922	820.000	66.084	79.942	37.951

[a] Values at this temperature were calculated with graphically extrapolated heat capacities.

TABLE 11. Experimental $C^{II}_{x,m}/R$ values for 2-aminobiphenyl
($R = 8.31451\ J \cdot K^{-1} \cdot mol^{-1}$)

mass / g	0.017159	0.009323	0.022312
Vol. cell / cm^3 [a]	0.05576	0.05387	0.05576
T/K	$C^{II}_{x,m}/R$	$C^{II}_{x,m}/R$	$C^{II}_{x,m}/R$
315.0	36.6	36.6	
335.0	37.4	36.8	37.6
355.0	38.2	38.6	38.2
375.0	39.1	39.6	39.4
395.0	40.6	40.6	40.4
415.0	41.6	41.6	41.3
435.0	42.7	42.6	42.4
455.0	43.7	43.9	43.4
475.0	45.3	45.1	44.8
495.0	46.1	46.3	46.0
515.0	47.2	47.7	47.1
535.0	48.5	49.1	48.3
555.0	49.8	50.6	49.6
575.0	51.1	52.2	50.8
595.0	52.4	53.8	52.0
615.0	53.6	55.5	53.2
635.0	55.0	57.1	54.3
655.0	56.1	58.8	55.3
675.0	57.2	60.5	56.2
695.0	58.2	62.2	57.0
715.0	59.1	63.9	57.7
735.0	59.9	65.7	58.4
755.0	60.7	67.5	59.6
775.0	61.4	69.6	60.7
795.0	62.0	72.0	61.8

[a] Volume measured at 298.15 K

TABLE 12. Densities and temperatures for the conversion from two phases to a single phase for 2-aminobiphenyl

$\rho/(kg \cdot m^{-3})$	T/K
167.8	818.5
219.5	832.2
243.0	835.9
297.9	838.2
347.6	832.9
387.8	823.2

TABLE 13. Parameters for equations (14) and (15), critical constants and acentric factor for 2-aminobiphenyl

A	2.69046	b_0	−0.43857
B	−1.66996	b_1	−1.65806
C	1.09246	b_2	3.59169
		b_3	−3.67273

T_c	838 K	p_c	3933 kPa	ρ_c	285 kg·m^{-3}	ω	0.456

TABLE 14. Values of $C^{II}_{V,m}(\rho = \rho_{sat})/R$ and $C_{sat,m}/R$ for 2-aminobiphenyl ($R = 8.31451\ J \cdot K^{-1} \cdot mol^{-1}$)

T/K	$C^{II}_{V,m}(\rho = \rho_{sat})/R$	$C_{sat,m}/R$	T/K	$C^{II}_{V,m}(\rho = \rho_{sat})/R$	$C_{sat,m}/R$
320.0	36.9	36.9	580.0	50.5	50.6
340.0	37.9	37.9	600.0	51.6	51.6
360.0	38.9	38.9	620.0	52.6	52.6
380.0	39.8	39.8	640.0	53.5	53.6
400.0	40.8	40.8	660.0	54.3	54.5
420.0	41.8	41.8	680.0	55.0	55.2
440.0	42.9	42.9	700.0	55.5	55.9
460.0	43.9	43.9	720.0	55.9	56.5
480.0	45.0	45.0	740.0	56.2	57.0
500.0	46.1	46.1	760.0	56.3	57.6
520.0	47.2	47.2	780.0	56.4	58.5
540.0	48.3	48.3	800.0	56.5	60.3
560.0	49.4	49.5	820.0	57.1	66.1

TABLE 15. Thermodynamic properties of 2-aminobiphenyl in the ideal-gas state. ($R = 8.31451\ J{\cdot}K^{-1}{\cdot}mol^{-1}$ and $p^\circ = 101.325$ kPa)

$\frac{T}{K}$	$\frac{\Delta_0^T H_m^\circ}{RT}$	$\frac{\Delta_{imp}H_m^\circ}{RT}$ [a]	$\frac{\Delta_0^T S_m^\circ}{R}$	$\frac{\Delta_{imp}S_m^\circ}{R}$ [b]	$\frac{\Delta_f H_m^\circ}{RT}$	$\frac{\Delta_f S_m^\circ}{R}$	$\frac{\Delta_f G_m^\circ}{RT}$
298.15 [c]	50.36±0.04	0.00	50.99±0.05	0.00	74.39±0.22	−55.19±0.05	129.58±0.22
300.00 [c]	50.20±0.04	0.00	51.13±0.05	0.00	73.87±0.22	−55.24±0.05	129.12±0.22
320.00 [c]	48.58±0.03	0.00	52.70±0.04	0.00	68.66±0.20	−55.86±0.04	124.52±0.20
340.00 [c]	47.22±0.03	0.00	54.24±0.04	0.00	64.08±0.19	−56.42±0.04	120.50±0.19
360.00	46.08±0.02	0.00	55.77±0.04	0.00	60.02±0.18	−56.93±0.04	116.95±0.18
380.00	45.14±0.02	0.00	57.29±0.04	0.00	56.41±0.17	−57.40±0.04	113.81±0.17
400.00	44.35±0.02	0.00	58.80±0.04	0.00	53.18±0.16	−57.82±0.04	111.00±0.17
420.00	43.71±0.02	0.01	60.31±0.05	0.01	50.27±0.15	−58.20±0.05	108.47±0.16
440.00	43.18±0.03	0.01	61.80±0.05	0.01	47.66±0.15	−58.54±0.05	106.20±0.15
460.00	42.76±0.03	0.02	63.29±0.05	0.02	45.29±0.14	−58.84±0.05	104.13±0.15
480.00	42.43±0.04	0.03	64.77±0.06	0.02	43.14±0.14	−59.11±0.06	102.25±0.15
500.00	42.18±0.06	0.05	66.25±0.08	0.04	41.19±0.14	−59.34±0.08	100.53±0.16
520.00	41.99±0.08	0.07	67.71±0.09	0.05	39.40±0.14	−59.55±0.09	98.95±0.17
540.00	41.87±0.09	0.10	69.17±0.11	0.07	37.77±0.15	−59.72±0.11	97.49±0.18
560.00	41.80±0.11	0.13	70.63±0.13	0.10	36.28±0.16	−59.87±0.13	96.14±0.19
580.00	41.78±0.13	0.17	72.08±0.15	0.13	34.91±0.17	−59.98±0.15	94.89±0.21
600.00	41.80±0.14	0.23	73.51±0.17	0.17	33.65±0.18	−60.08±0.17	93.73±0.23
620.00	41.85±0.16	0.29	74.94±0.19	0.21	32.49±0.19	−60.15±0.19	92.64±0.24
640.00 [c]	41.94±0.18	0.36	76.36±0.21	0.27	31.41±0.21	−60.21±0.21	91.62±0.26
660.00 [c]	42.04±0.20	0.44	77.76±0.23	0.33	30.42±0.22	−60.25±0.23	90.66±0.28
680.00 [c]	42.16±0.22	0.54	79.15±0.25	0.40	29.48±0.24	−60.28±0.25	89.76±0.30
700.00 [c]	42.29±0.24	0.65	80.51±0.28	0.48	28.61±0.26	−60.30±0.28	88.91±0.32
720.00 [c]	42.41±0.27	0.77	81.84±0.30	0.58	27.77±0.28	−60.33±0.30	88.10±0.33
740.00 [c]	42.53±0.29	0.91	83.13±0.33	0.68	26.96±0.30	−60.37±0.33	87.34±0.35
760.00 [c]	42.62±0.31	1.06	84.38±0.35	0.80	26.18±0.33	−60.43±0.35	86.61±0.37
780.00 [c]	42.69±0.34	1.23	85.58±0.38	0.94	25.39±0.35	−60.53±0.38	85.92±0.39
800.00 [c]	42.71±0.37	1.42	86.71±0.41	1.09	24.60±0.38	−60.66±0.41	85.25±0.41
820.00 [c]	42.67±0.41	1.63	87.77±0.45	1.26	23.77±0.41	−60.84±0.45	84.62±0.43

[a] Gas-imperfection correction to the ideal-gas enthalpy.

[b] Gas-imperfection correction to the ideal-gas entropy.

[c] Values at this temperature were calculated with extrapolated vapor pressures calculated from the fitted Cox coefficients.

TABLE 16 Gibbs energies of formation [a]
(R = 8.31451 $J \cdot K^{-1} \cdot mol^{-1}$ and p° = 101.325 kPa)

T/K	$\Delta_f G^\circ_m$ /RT			
	fluorene	carbazole	dibenzofuran	
400	98.09	106.69	55.29	
500	87.39	94.84	52.43	
600			50.67	
700			49.46	
	2-methylbiphenyl	2-aminobiphenyl	2-hydroxybiphenyl	biphenyl
400	97.39	111.00	50.26	94.99
500	88.95	100.53	50.61	84.62
600	83.54	93.73	50.99	77.89
700	79.73	88.91	51.30	73.14
	methane	ammonia	water	
400	−12.67	−1.72	−67.33	
500	−7.90	1.21	−52.70	
600	−4.62	3.22	−42.91	
700	−2.20	4.71	−35.89	

[a] See Appendix 1 for details on the derivations of the listed values.

TABLE 17. Gibbs energies of reactions [a]
($R = 8.31451\ J \cdot K^{-1} \cdot mol^{-1}$ and $p^\circ = 101.325\ kPa$)

T/K	$-\Delta_r G^\circ_m / RT$			
Reaction # / T/K	1	2	3	4
400	0.70	15.07	−4.31	17.73
500	−1.56	12.23	−5.69	14.70
600		10.27		12.62
700		8.79		11.06

Reaction # / T/K	5	6
400	5.03	22.60
500	1.82	18.69
600	−0.32	16.01
700	−1.84	14.05

[a] See table 18 for reaction corresponding to each number.

TABLE 18. Equations to represent the equilibria shown in figure 5

Reaction #	Reaction
1	FLUORENE → 2-METHYLBIPHENYL $\ln K' = 4520/T - 10.60 + [\ln(P_{H_2} / P^\circ)]$
2	2-METHYLBIPHENYL → BIPHENYL + METHANE $\ln K' = 5845/T - 0.49 + [\ln(P_{H_2} / P^\circ)]$
3	CARBAZOLE → 2-AMINOBIPHENYL $\ln K' = 2760/T - 11.21 + [\ln(P_{H_2} / P^\circ)]$
4	2-AMINOBIPHENYL → BIPHENYL + AMMONIA $\ln K' = 6210/T - 2.24 + [\ln(P_{H_2} / P^\circ)]$
5	DIBENZOFURAN → 2-HYDROXYBIPHENYL $\ln K' = 6414/T - 11.01 + [\ln(P_{H_2} / P^\circ)]$
6	2-HYDROXYBIPHENYL → BIPHENYL + WATER $\ln K' = 7970/T - 2.70 + [\ln(P_{H_2} / P^\circ)]$

APPENDIX 1.

LISTING OF AUXILIARY THERMODYNAMIC PROPERTY MEASUREMENT SOURCES

GENERAL DETAILS

Enthalpies and entropies for equilibrium hydrogen, oxygen, and nitrogen used in the derivation of the ideal-gas thermodynamic properties of each compound were determined from JANAF tables.[A1] Enthalpies and entropies for graphite were determined with the polynomial[A2] used to calculate the values from 298.15 K to 6000 K listed in the JANAF tables. Values for the enthalpies of formation for $CO_2(g)$ and $H_2O(l)$ used to derive enthalpies of formation for each compound were those listed by CODATA.[A3] Details of the sources and/or methods of estimation of the ideal-gas thermodynamic properties of each compound follow. The ideal-gas Gibbs energies of formation for methane, ammonia, and water used in the calculations were determined from the JANAF tables.[A1] The derived values for the Gibbs energies of formation are reported in table 16 of the main text. Uncertainty intervals (one standard deviation) in the estimated Gibbs energies of formation reported in table 16 vary, depending on the degree of estimation used in the derivations. Since the values were used to determine Gibbs energies of reaction in a closed system (in the thermodynamic sense), the uncertainties in the enthalpies and entropies of the elements cancel in the equilibrium calculations. By neglecting the uncertainties in the elements, the uncertainty interval for the dimensionless Gibbs energies of formation (i.e., $\Delta_f G^\circ_m/RT$) for each compound listed in table 16 probably lies in the range ±0.2 to ±0.5.

FLUORENE

The condensed-phase thermodynamic properties for fluorene in the temperature range 11 to 427 K were reported in reference A4. Vapor-pressure measurements in the temperature ranges 348 to 387 K (solid phase) and 395 K to 626 K (liquid phase) have been completed at NIPER. The solid-phase measurements were reported,[A5] but the liquid-phase measurements are unpublished at present. The values were used to derive the ideal-gas enthalpies and entropies of fluorene at 400 and 500 K. The derived ideal-gas enthalpies and entropies were combined with the condensed-phase enthalpy of combustion[A6] and the enthalpies of formation for $CO_2(g)$ and $H_2O(l)$ given by CODATA[A3] to calculate the corresponding enthalpies, entropies, and Gibbs energies of formation. Further measurements are in progress [funded by the DOE Advanced Research/Coal Liquefaction program] to extend the range of the thermodynamic properties of fluorene to at least 800 K.

CARBAZOLE

Due its high melting point (521 K) direct thermodynamic-property measurements on carbazole are not possible in the available apparatus at NIPER. However, with the availability of measurements on 9-methylcarbazole (a liquid at room temperature) and 1-methylpyrrole, reliable values for carbazole itself can be estimated. As can be seen in the following figure, the molecular environment of each atom within the balanced equation is approximately the same, maintaining the rules of group additivity for property estimation.

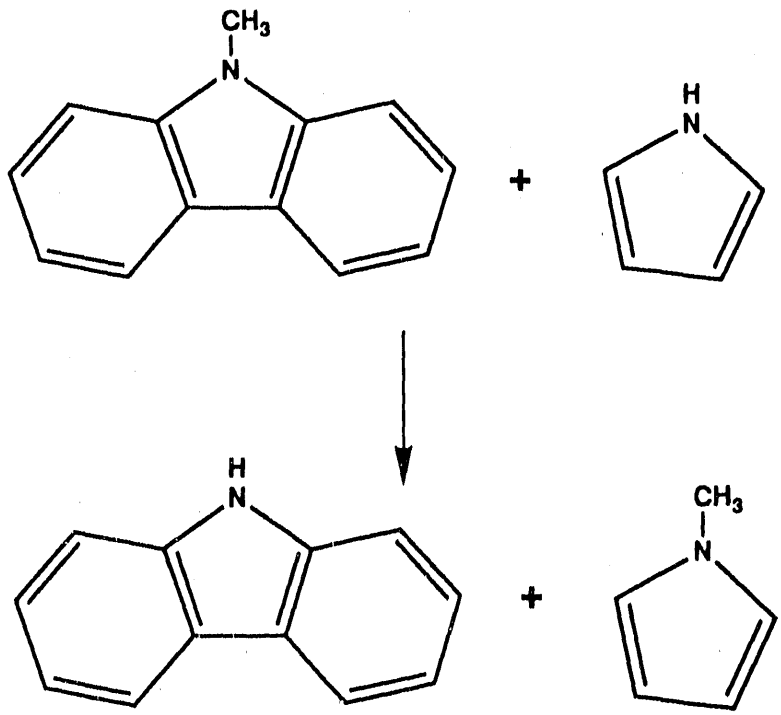

Condensed-phase thermodynamic properties for 9-methylcarbazole in the temperature range 13 to 388 K determined at NIPER were reported.[A7] Vapor-pressure measurements in the temperature range 373 to 673 K (liquid phase) have been completed at NIPER, but are unpublished at present. The values were used to derive the ideal-gas enthalpies and entropies of 9-methylcarbazole at 400 and 500 K. The derived ideal-gas enthalpies and entropies were combined with the condensed-phase enthalpy of combustion[A8] and the enthalpies of formation for $CO_2(g)$ and $H_2O(l)$ given by CODATA[A3] to calculate the corresponding enthalpies, entropies, and Gibbs energies of formation. Ideal-gas thermodynamic functions for 1-methylpyrrole in the temperature range 0 to 1000 K were reported.[A9]

The ideal-gas thermodynamic functions derived here for carbazole are in serious disagreement with those listed in the American Petroleum Institute (API) Monograph Series Publication 716.[A10] The ideal-gas thermodynamic functions reported in the monograph were derived using molecular-property data[A11] and vibrational frequencies.[A12] The vibrational frequencies are for the solid phase or from solution IR spectra and their use to calculate ideal-gas functions is not recommended. Detailed comparisons between the NIPER results and other literature values will be published in a future report.

DIBENZOFURAN

The thermodynamic functions for dibenzofuran determined at NIPER are reported.[A13]

2-METHYLBIPHENYL and 2-HYDROXYBIPHENYL

The thermodynamic functions for 2-methylbiphenyl and 2-hydroxybiphenyl have been measured at NIPER and will be the subject of a topical report within the DOE Advanced Research Liquefaction program.

BIPHENYL

The thermodynamic functions for biphenyl determined at NIPER are reported.[A14]

REFERENCES FOR APPENDIX

A1. Chase, M. W., Jr.; Davies, C. A.; Cowney, J. R.; Frurip, D. J.; McDonald, R. A.; Syverud, A. N. *JANAF Thermochemical Tables* Third edition. Supplement to *J. Phys. Chem. Ref. Data* **1985**, 14.

A2. Chirico, R. D.; Archer, D. G.; Hossenlopp, I. A.; Nguyen, A.; Steele, W. V.; Gammon, B. G. *J. Chem. Thermodynamics* **1990**, 22, 665.

A3. Cox, J. D.; Wagman, D. D.; Medvedev, V. A.: editors. *CODATA Key Values for Thermodynamics.* Hemisphere: New York. **1989.**

A4. Finke, H. L.; Messerly, J. F.; Lee, S. H.; Osborn, A. G.; Douslin, D. R. *J. Chem. Thermodynamics* **1977**, 9, 937.

A5. Osborn, A. G.; Douslin, D. R. *J. Chem. Eng. Data* **1975**, 20, 229.

A6. Unpublished NIPER data referred to in reference A3.

A7. Messerly, J. F.; Todd, S. S.; Finke, H. L.; Good, W. D.; Gammon, B. E. *J. Chem. Thermodynamics* **1988**, 20, 209.

A8. Good, W. D. *J. Chem. Eng. Data* **1972**, 17, 28.

A9. Steele, W. V.; Chirico, R. D.; Collier, W. B.; Hossenlopp, I. A.; Nguyen, A.; Strube, M. M. *Thermochemical and Thermophysical Properties of Organic Nitrogen Compounds found in Fossil Materials.* NIPER-188. Published by DOE Fossil Energy, Bartlesville Project Office. Available from NTIS Report No. DE-8687001252, November **1986.**

A10. Kudchadker, A. P.; Kudchadker, S. A.; Wilhoit, R. C.; Gupta, S. K. *Carbazole* API Monograph Series Publication 716. American Petroleum Institute, Washington, D.C. June **1981.**

A11. Kurshashi, M.; Fukuyo, M.; Shimoda, A.; Fursaki, A.; Nitta, I. *Bull. Chem. Soc. Japan* **1969**, 42, 2174.

A12. Bree, A.; Zwarich, R. *J. Chem. Phys.* **1968**, 49, 3344.

A13. Chirico, R. D.; Gammon, B. E.; Knipmeyer, S. E.; Nguyen, A.; Strube, M. M.; Tsonopoulos, C.; Steele, W. V. *J. Chem. Thermodynamics* In press.

A14. Chirico, R. D.; Knipmeyer, S. E.; Nguyen, A.; Steele, W. V. *J. Chem. Thermodynamics* **1989**, 21, 1307.

★U.S. GOVERNMENT PRINTING OFFICE: 1990 -561 -029/20056

END

DATE FILMED

03/05/91